

2009

Use of novel assays to measure in vivo base excision DNA repair

Preethi Sundaresakumar
San Jose State University

Follow this and additional works at: https://scholarworks.sjsu.edu/etd_theses

Recommended Citation

Sundaresakumar, Preethi, "Use of novel assays to measure in vivo base excision DNA repair" (2009).
Master's Theses. 3681.
DOI: <https://doi.org/10.31979/etd.5cd3-pbbv>
https://scholarworks.sjsu.edu/etd_theses/3681

This Thesis is brought to you for free and open access by the Master's Theses and Graduate Research at SJSU ScholarWorks. It has been accepted for inclusion in Master's Theses by an authorized administrator of SJSU ScholarWorks. For more information, please contact scholarworks@sjsu.edu.

USE OF NOVEL ASSAYS TO MEASURE IN VIVO BASE EXCISION DNA REPAIR

A Thesis

Presented to

The Faculty of the Department of Biological Sciences

San José State University

In Partial Fulfillment

of the Requirements for the Degree

Master of Science

by

Preethi Sundaresakumar

May 2009

UMI Number: 1470953

INFORMATION TO USERS

The quality of this reproduction is dependent upon the quality of the copy submitted. Broken or indistinct print, colored or poor quality illustrations and photographs, print bleed-through, substandard margins, and improper alignment can adversely affect reproduction.

In the unlikely event that the author did not send a complete manuscript and there are missing pages, these will be noted. Also, if unauthorized copyright material had to be removed, a note will indicate the deletion.



UMI Microform 1470953
Copyright 2009 by ProQuest LLC
All rights reserved. This microform edition is protected against
unauthorized copying under Title 17, United States Code.

ProQuest LLC
789 East Eisenhower Parkway
P.O. Box 1346
Ann Arbor, MI 48106-1346

© 2009

Preethi Sundaresakumar

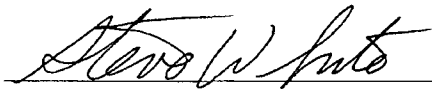
ALL RIGHTS RESERVED

SAN JOSÉ STATE UNIVERSITY

The Undersigned Thesis Committee Approves the Thesis Titled
USE OF NOVEL ASSAYS TO MEASURE IN VIVO BASE EXCISION DNA REPAIR

by
Preethi Sundaresakumar

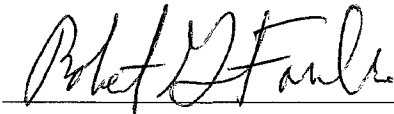
APPROVED FOR THE DEPARTMENT OF BIOLOGICAL SCIENCES



3/18/09

Dr. Steven White, Department of Biological Sciences

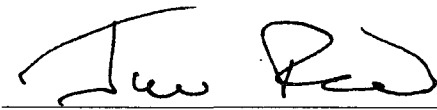
Date



3/18/09

Dr. Robert Fowler, Department of Biological Sciences

Date

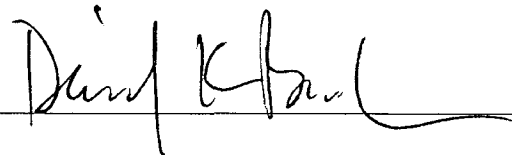


3/18/09

Dr. James Ford, Stanford University

Date

APPROVED FOR THE UNIVERSITY



5/5/09

Associate Dean Office of Graduate Studies and Research

Date

ABSTRACT

USE OF NOVEL ASSAYS TO MEASURE IN VIVO BASE EXCISION DNA REPAIR

by Preethi Sundaresakumar

Oxidative DNA damage due to reactive oxygen species (ROS) can cause single-base alterations such as 8-oxo-7,8-dihydroguanine (8oxodG) lesions, which are repaired by the base excision DNA repair (BER) pathway. Assays developed to date, to measure BER, are limited by in vitro analysis and use of radiolabeled reagents. This thesis outlines the design of a novel assay to measure the kinetics of BER in vivo, using a biotin-tagged oligonucleotide DNA substrate that contains an 8oxodG lesion. The substrate DNA is transfected into target cells and incubated to allow repair of the lesions. The DNA is then captured following cell lysis and the disappearance of 8oxodG lesions is monitored using competitive 8oxodG ELISA. This assay was developed to corroborate the results obtained from our investigations on the role of the breast cancer susceptibility protein-1 (BRCA1) in BER, using another novel in vivo assay called the host-cell reactivation (HCR) assay. Preliminary results from this study showed that BRCA1 is involved in BER. Together, these in vivo assays may be used to identify potential cancer genes that regulate the BER pathway.

ACKNOWLEDGEMENTS

I express my heartfelt gratitude to Dr. James Ford, for giving me the opportunity to conduct research in his laboratory, and for his invaluable guidance, constant encouragement, and patience. It has been a great learning experience and a pleasure to work under his guidance. I sincerely thank Dr. Steven White and Dr. Robert Fowler for rendering their valuable suggestions during the preparation of this thesis.

I express my profound gratitude to Dr. Elizabeth Alli for her immeasurable support, guidance, and inspiration at every stage of this thesis. I also thank Dr. Lisa McPherson, Dr. Kedar Hastak, and Dr. Patrick Linn for their encouragement, suggestions and technical assistance. Last, but not the least, I express my utmost gratitude to my husband Mahesh for his relentless support and encouragement.

TABLE OF CONTENTS

| | |
|--|-----|
| LIST OF FIGURES..... | vii |
| LIST OF TABLES..... | ix |
| LIST OF ABBREVIATIONS..... | x |
| INTRODUCTION..... | 1 |
| CHAPTER ONE: | |
| INVESTIGATION ON THE ROLE OF BRCA1 IN BER USING THE HOST-CELL REACTIVATION ASSAY..... | 9 |
| Introduction..... | 9 |
| Materials and methods..... | 13 |
| Results..... | 24 |
| Discussion..... | 29 |
| CHAPTER TWO: | |
| DEVELOPMENT OF A NOVEL ASSAY TO MEASURE IN VIVO BER..... | 33 |
| Introduction..... | 33 |
| Materials and methods..... | 38 |
| Results..... | 47 |
| Discussion..... | 73 |
| CONCLUSION..... | 82 |
| REFERENCES..... | 83 |

LIST OF FIGURES

| FIGURE | TITLE | PAGE |
|--------|---|------|
| 1. | Chemical formula of 8-oxo-7,8-dihydroguanine..... | 4 |
| 2 | Base excision repair of 8oxodG lesions in mammalian cells..... | 8 |
| 3 | Overview of the host-cell reactivation assay to measure BER of 8oxodG lesions..... | 19 |
| 4. | Restriction analysis of the plasmids isolated from bacterial clones transformed with the wild-type <i>BRCA1</i> or pcDNA3.0 constructs..... | 25 |
| 5 | Western blot analysis of nuclear extracts from MCF7 and SUM149PT cells transfected with wild-type <i>BRCA1</i> or the empty vector constructs..... | 26 |
| 6 | Relative GFP expression from the HCR assay to measure BER in SUM149PT cells transfected with wild-type <i>BRCA1</i> or empty vector constructs..... | 28 |
| 7 | Overview of the in vivo 8oxodG BER assay..... | 48 |
| 8 | Gel analysis of the single-stranded DNA oligonucleotides used in the in vivo 8oxodG BER assay..... | 49 |
| 9 | Gel analysis of the annealed double-stranded substrate and control DNA.... | 51 |
| 10 | Specificity of the 8oxodG ELISA at different assay conditions..... | 54 |
| 11 | Efficiency of the 8oxodG competitive ELISA..... | 56 |

LIST OF FIGURES

| FIGURE | TITLE | PAGE |
|--------|--|------|
| 12 | Dose-dependent detection of 8oxodG lesions on the +8oxodG DNA in the presence of the -8oxodG DNA..... | 60 |
| 13 | Titration of the amount of streptavidin-coated magnetic beads required to capture the control DNA..... | 62 |
| 14 | Selection of a suitable transfection reagent for the BER assay | 65 |
| 15 | Optimal volume of Lipofectamine™ 2000 for use in the transfection step of the BER assay | 66 |
| 16 | Transfection of control and substrate DNA into SUM149PT and MCF7 cells..... | 69 |
| 17 | Quantification of 8oxodG lesions on the +8oxodG DNA in the presence or absence of the biotinylated DNA..... | 72 |

LIST OF TABLES

| TABLE | TITLE | PAGE |
|-------|---|------|
| 1 | Designation of wells for the plating, transfection, and infection of SUM149PT cells in the HCR assay..... | 21 |
| 2 | Amount of +8oxodG and -8oxodG DNA used for the in vitro validation of the 8oxodG ELISA..... | 59 |
| 3 | Amount of biotinylated DNA and/or +8oxodG DNA used to determine the efficiency of the 8oxodG ELISA | 71 |

LIST OF ABBREVIATIONS

| | |
|-----------------|---|
| 8oxodG | 8-oxo-7,8-dihydroguanine |
| Ad-GFP | Recombinant adenovirus carrying a GFP reporter gene |
| AP | Apurinic/apyrimidic |
| APE1 | Apurinic/apyrimidic endonuclease 1 |
| BER | Base excision repair |
| BSA | Bovine serum albumin |
| CO ₂ | Carbon dioxide |
| DMSO | Dimethyl sulfoxide |
| EDTA | Ethylenediaminetetraacetic acid |
| EGTA | Ethylene-glycol tetraacetic acid |
| ELISA | Enzyme linked immunosorbant assay |
| ER | Estrogen receptor |
| FBS | Fetal bovine serum |
| FITC | Fluorescein isothiocyanate |
| GFP | Green fluorescent protein |
| GGR | Global genomic repair |
| HCR | Host-cell reactivation assay |
| HEPES | 4-(2-hydroxyethyl)-1-piperazineethanesulfonic acid |
| HER | Human epidermal growth factor receptor-2 |
| hOGG1 | Human 8-hydroxyguanine DNA-glycosylase |
| HPLC-ECD | High performance liquid chromatography with electrochemical detection |
| HR | Homologous recombination |
| HRP | Horseradish peroxidase |
| kb | kilobase |
| kDa | kiloDalton |
| LB | Luria-Bertani broth |
| LP-BER | Long-patch base excision repair |

| | |
|----------|---|
| MMR | Mismatch repair |
| MTH1 | MutT homolog 1 |
| MTT | 3-(4,5-dimethylthiazol-2-yl)-2,5-diphenyl tetrazolium bromide |
| MUTYH | MutY homolog |
| NaCl | Sodium chloride |
| NaOH | Sodium hydroxide |
| NER | Nucleotide excision repair |
| NHEJ | Nonhomologous end-joining |
| NLS | Nuclear-localization signals |
| P/S/F | Penicillin/streptomycin/fungizone |
| PBS | Phosphate-buffered saline |
| PBST | Phosphate-buffered saline Tween-20 |
| PCNA | Proliferating cell nuclear antigen |
| PR | Progesterone receptor |
| PVDF | Polyvinylidene fluoride |
| RING | Really Interesting New Gene |
| ROS | Reactive oxygen species |
| SCD | SQ cluster domain |
| SDS | Sodium dodecyl sulfate |
| SP-BER | Short-patch base excision repair |
| TAE | Tris- acetate EDTA |
| TBE | Tris-borate-EDTA |
| TBP | TATA-binding protein |
| TCR | Transcription-coupled repair |
| TE | Tris-EDTA |
| TEG | Tetra-ethyleneglycol |
| TMB | 3,3',5,5' - tetramethylbenzidine |
| Tris-HCl | Tris-Hydrochloride |
| UV | Ultraviolet |

INTRODUCTION

Cellular DNA constantly faces assault from various endogenous and exogenous agents. Nucleotides are oxidized on exposure to reactive oxygen species (ROS) which are generated endogenously during various cellular metabolic processes (Friedberg et al., 2006a, chap. 2). Oxidized guanine products such as 8-oxo-7,8-dihydroguanine (8oxodG) are common ROS-induced single base alterations. Unless repaired, oxidative DNA damage results in genetic instability and tumorigenesis. The base excision DNA repair (BER) pathway is the major cellular pathway that corrects oxidation-induced single base alterations (David, O'Shea, & Kundu, 2007; Dizdaroglu, 2005; Mitra, Boldogh, Izumi, & Hazra, 2001; Seeberg, Eide, & Bjørås, 1995).

A number of assays have been developed to monitor BER activity. These assays have been used to identify the various steps and the proteins involved in the pathway. In addition, they allow comparison of repair activity in different cell types following exposure to oxidative stress. However, such assays are limited due to the need for in vitro analyses using cell extracts and the use of radiolabeled reagents.

In this study, we have designed a novel assay to measure BER of 8oxodG lesions in vivo, and optimized the working conditions for some of the steps in the assay. This assay measures the repair of a short double-stranded oligonucleotide DNA substrate carrying a single 8oxodG lesion on one strand and a 3' biotin tag on the complementary strand. Following transfection of the substrate DNA into target cells and incubation to allow time for repair, the cells are lysed, and the biotin-tagged substrate DNA is captured

using streptavidin-coated magnetic beads. The 8oxodG lesions on the substrate DNA are then quantified using a competitive 8oxodG enzyme-linked immunosorbent assay (ELISA). The amount of 8oxodG lesions quantified is inversely proportional to the efficiency of BER in the cells.

The *in vivo* BER assay was designed to corroborate the preliminary results obtained from another study conducted as part of this thesis. This study involved the investigation of the role of the breast cancer susceptibility protein-1 (BRCA1) in the BER pathway, using a novel *host-cell reactivation assay* (HCR) for BER that was recently developed in our laboratory. This assay for BER monitors the ability of cells in culture to remove transcription-blocking 8oxodG lesions introduced *ex-vivo* into a green fluorescent protein (GFP) reporter gene in a recombinant adenovirus. Repair of the 8oxodG lesions by the cellular BER pathway allows for expression of GFP, which can be measured using standard fluorescence detection methods. In our study, a wild-type *BRCA1* expression vector was transfected into *BRCA1* deficient cells, and the cells were subjected to the HCR assay. Preliminary results show that the BRCA1 protein enhances the BER pathway.

This thesis has been divided into two chapters. In the first chapter, the preliminary investigations on the role of the BRCA1 protein in BER using the HCR assay have been described. In the second chapter, the development of a novel assay to measure the *in vivo* BER of 8oxodG lesions has been described. In the following section, an overview of oxidative DNA damage, 8oxodG lesions, and the BER pathway has been provided, to serve as an introduction to the two chapters that follow.

Oxidative DNA Damage

Cellular DNA is susceptible to oxidation by ROS and transition metals (Neely & Essigmann, 2006). In the cell, ROS are by-products of aerobic metabolism. They are also generated during metabolism of xenobiotic compounds (Park et al., 2005) and phagocytosis (Bogdan, Rölinghoff, & Diefenbach, 2000). ROS may also be introduced exogenously by radiation, redox cycling compounds, drugs, or cigarette smoke (Friedberg et al., 2006a, chap. 2). Different types of ROS include superoxide ($O_2^{\cdot-}$), hydroxyl (OH^{\cdot}), peroxy (RO_2^{\cdot}), alkoxy (RO^{\cdot}), hydroperoxy (HO_2^{\cdot}), singlet oxygen (1O_2), peroxynitrite ($ONOO^-$), and hydrogen peroxide (H_2O_2). A cell usually decreases ROS levels using free radical scavengers and antioxidant enzymes (Pacifi & Davies, 1991). When these defenses fail, elevated ROS levels cause damage to nucleic acids, proteins, carbohydrates, and lipids in a cell (Friedberg et al., 2006a, chap. 2).

ROS induce the formation of a plethora of DNA oxidation products (Bjelland & Seeberg, 2003), some of which are 8oxodG, thymine glycol, formaminopyrimidine, and 5-hydroxycytosine. It is usually the electrophilic carbon centers of the bases that are oxidized (Nilsen & Kroken, 2001). If left unrepaired, oxidized bases lead to apurinic/apyrimidic (AP) sites and strand breaks (Friedberg et al., 2006a, chap. 2), and result in DNA mutations, genetic instability, and cancer. Oxidized bases and AP sites are mainly repaired using the BER pathway (Seeberg et al., 1995). Some oxidative lesions also appear to be repaired by the nucleotide excision repair (NER) and mismatch repair (MMR) pathways (Bjelland & Seeberg, 2003). Strand breaks may be repaired by homologous recombination (HR) or non-homologous end-joining (NHEJ) mechanisms.

8-oxo-7,8-dihydroguanine (8oxodG)

Among the ROS-induced DNA oxidation products, guanine oxidation products occur most frequently. This is because guanine, owing to its low reduction potential ($E_7 = 1.29$ V) (Neely & Essigmann, 2006; Steenken & Jovanovic, 1997), is more susceptible to oxidation (Bjelland & Seeberg, 2003). A guanine oxidation product that has been thoroughly examined and is often used as a biomarker of cellular oxidative stress is 8oxodG (David et al., 2007) (Figure 1).

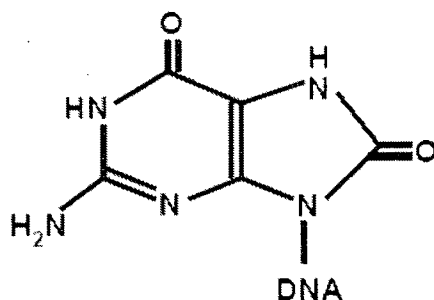


Figure 1. Chemical formula of 8-oxo-7,8-dihydroguanine.

8oxodG lesions are highly stable and mutagenic. Their stability is evidenced by the fact that these lesions were detected among eight oxidative base modifications in ancient DNA (Höss, Jaruga, Zastawny, Dizdaroglu, & Pääbo, 1996). In the *anti* conformation, they form 8oxodG (*anti*) – C (*anti*) base pair. However, in the *syn* conformation, they mimic thymidine and thus form a stable 8oxodG (*syn*) – A (*anti*) base pair (David et al., 2007). Such base pairing specificities allow bypass of 8oxodG lesions by replicative DNA polymerases (Shibutani, Takeshita, & Grollman, 1991) and this

ultimately results in GC to TA transversion mutations (Cheng, Cahill, Kasai, Nishimura, & Loeb, 1992). In humans, a set of three enzymes (called the GO system) are involved in the repair of 8oxodG lesions. The enzyme MutT homolog 1 (MTH1) hydrolyzes 8oxodGTP bases from the nucleotide pool, thereby preventing their incorporation into DNA. The human 8-hydroxyguanine DNA glycosylase (hOGG1), functions in the first step of the BER pathway to specifically detect and excise the 8oxodG lesion from the 8oxodG-C base pair. If 8oxodG is not removed by hOGG1, then following replication, the 8oxodG base pairs with adenine. The enzyme MutY homolog (MUTYH) then removes the adenine from the 8oxodG-A base pair, and allows the incorporation of a cytosine opposite the 8oxodG base. This provides another opportunity for the hOGG1 enzyme to excise the 8oxodG lesion (Friedberg et al., 2006b, chap. 6).

Base Excision DNA Repair (BER)

To deal with the constant assaults faced by cellular DNA, repair pathways have evolved, each specializing in the correction of certain types of damage. The BER pathway, first discovered by Tomas Lindahl in 1974, specializes in the repair of small base alterations that do not distort the DNA helix (Fromme & Verdine, 2004). Besides oxidized bases, the BER pathway also recognizes and repairs alkylated bases (formed due to base exposure to S-adenosylmethionine and tobacco-specific nitosamines), AP sites (formed by the spontaneous loss of purines from DNA) and deaminated bases (resulting from hydrolytic deamination of amine-containing DNA bases) (Fromme & Verdine, 2004).

The BER system consists of a group of lesion-specific enzymes termed DNA glycosylases, which recognize and excise specific base modifications, resulting in AP sites. Other enzymes act in a series of steps to fill in the missing base, and ultimately restore the correct sequence (Krokan, Nilsen, Skorpen, Otterlei, & Slupphaug, 2000). Since the focus of this thesis is on the repair of oxidized bases (particularly 8oxodG), a brief description of the steps involved in the BER of 8oxodG lesions is given below.

The hOGG1 glycosylase is the mammalian DNA glycosylase that recognizes and excises the 8oxodG lesion from 8oxodG-C base pairs. The enzyme removes 8oxodG lesions via displacement using a nucleophile active-site residue, which is an amine (Fromme & Verdine, 2004). Following displacement of 8oxodG, hOGG1 catalyses the cleavage of the N-glycosyl bond between the lesion and deoxyribose in the backbone, resulting in an AP site. Being a bifunctional DNA glycosylase, hOGG1 has both DNA glycosylase and DNA lyase activities. Thus, following removal of the 8oxodG lesion, the lyase activity allows the enzyme to cleave the DNA backbone on the 3' side of the lesion resulting in the generation of a 3'- α , β -unsaturated aldehyde end and a 5' phosphate end. The human apurinic/apyrimidic endonuclease 1 (APE1) then removes the 3'- α , β -unsaturated aldehyde by virtue of its 3'-phosphodiesterase activity. This results in a single nucleotide gap that is flanked by 3' hydroxyl and 5' phosphate ends. DNA polymerase β then fills the gap and the strand is resealed by DNA ligase III and X-ray Repair Complementing Defective Repair in Chinese Hamster Cells 1 (XRCC1) heterodimers (Figure 2A) (Friedberg et al., 2006b, chap. 6; Fromme & Verdine, 2004; Hirano, 2008).

Studies have shown that in the presence of APE1, the hOGG1 lyase activity is bypassed (Vidal, Hickson, Boiteux, & Radicella, 2001). APE1 then directly cleaves the backbone at the 5' side of the AP site resulting in the formation of a 3' hydroxyl end and a 5' deoxyribose phosphate (dRP) end. Beyond this step, repair can proceed in one of two alternative pathways which involve either the replacement of one (short-patch BER) or more nucleotides (long-patch BER) at the lesion site (Fortini et al., 2003). It has been shown that hOGG1-mediated repair of 8oxodG occurs almost exclusively along the short-patch pathway (Fortini, Parlanti, Sidorkina, Laval, & Dogliotti, 1999). In short-patch BER (SP-BER), following cleavage by APE1, DNA polymerase β removes the 5'-dRP due to its intrinsic dRPase activity and then fills in the gap due to its DNA polymerase activity. The strand is then resealed by DNA ligase III and XRCC1 heterodimers, or DNA ligase I (Figure 2B) (Friedberg et al., 2006b, chap. 6; Fromme & Verdine, 2004).

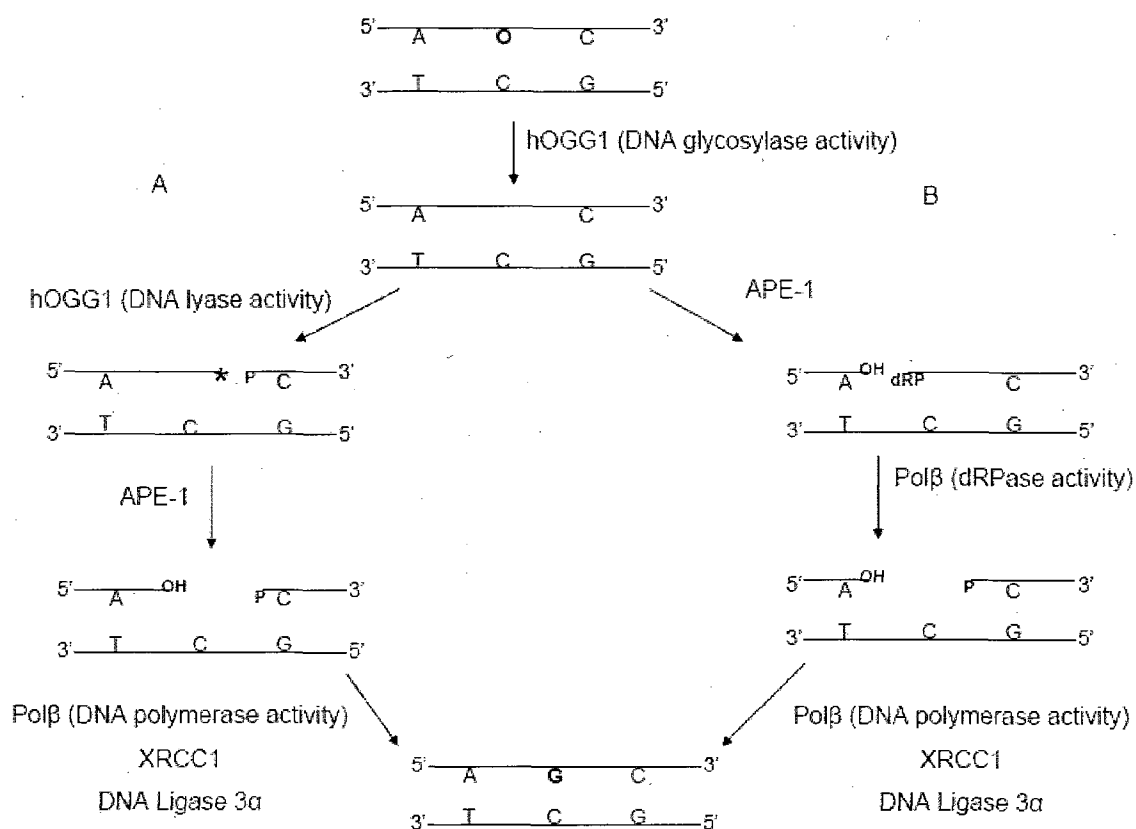


Figure 2. Base excision repair of 8oxodG lesions in mammalian cells. The hOGG1 enzyme excises the 8oxodG base (O) in an 8oxodG-C base pair, resulting in an AP site. Using its lyase activity (A), the enzyme then cleaves the DNA backbone on the 3' side of the lesion resulting in the generation of a 3'-α, β-unsaturated aldehyde end (*) and a 5' phosphate (P) end. The APE1 enzyme then removes the 3'-α, β-unsaturated aldehyde, thereby creating a single nucleotide gap that is flanked by 3' hydroxyl (OH) and 5' phosphate (P) ends. DNA polymerase β (Pol β) then fills the gap and the strand is resealed by a DNA ligase III/XRCC1 heterodimer. Alternatively (B), the hOGG1 lyase activity is bypassed and following 8oxodG base excision, APE1 directly cleaves the backbone at the 5' side of the AP site resulting in the formation of a 3' hydroxyl end (OH) and a 5' deoxyribose phosphate (dRP) end. Following cleavage by APE1, Pol β removes the 5'-dRP, and then fills in the single nucleotide gap. The strand is then resealed by the DNA ligase III and XRCC1 heterodimer or DNA ligase I.

CHAPTER ONE

INVESTIGATION ON THE ROLE OF BRCA1 IN BER USING THE HOST-CELL REACTIVATION ASSAY

Introduction

The Breast Cancer Susceptibility Gene-1 (BRCA1)

The *BRCA1* gene was mapped to chromosome 17q21 by Miki et al. in 1994. It contains 24 exons that encode a 220 kDa protein of 1863 amino acids. The protein consists of multiple functional domains; a highly conserved N-terminal Really Interesting New Gene-1 (RING) finger domain (residues 1-112), two centrally located nuclear-localization signals (NLS), an 'SQ' cluster domain (SCD) containing serine and glutamine residues (residues 1280-1524), and two BRCA1 carboxy terminal (BRCT) domains (residues 1646-1863) (Deng, 2006; Venkitaraman, 2001).

The BRCA1 protein functions as a tumor suppressor and has been implicated in a number of cellular activities such as cell cycle checkpoint control, centrosome duplication, chromatic remodeling and transcription, replication, recombination, DNA repair, ubiquitination and apoptosis (reviewed in Daniel, 2002; Deng, 2006; Scully, Xie, & Nagaraju, 2004; Starita & Parvin, 2003; Venkitaraman, 2001; Yarden & Papa, 2006). Deng (2006) proposed that a loss of these functions may be responsible for the gross genetic instability observed in *BRCA1*-mutated mouse and human mammary tumors

(Weaver et al., 2002; Xu et al., 1999). A study (Tirkkonen et al., 1997) also showed that *BRCA1*-associated breast cancers have high levels of chromosomal aneuploidy when compared to breast carcinomas lacking a *BRCA1* mutation. While on one hand, this genetic instability triggers DNA damage response pathways leading to growth arrest and activation of pro-apoptotic signals, on the other hand, the cell continues to accumulate mutations in critical tumor regulatory genes, including *p53*, *PTEN*, *Rb1*, *ErbB2*, *c-Myc*, *p27*, and *cyclin D1*, that initiate carcinogenesis (Brodie et al., 2001; Deng, 2006; Xu et al., 1999).

BRCA1-Associated Breast Cancers

Breast cancer is the second leading cause of cancer mortality in Western women (Deng, 2006). About 10% of breast cancer cases are heritable; the remaining being sporadic cases (Easton & Peto, 1990). Approximately 50% of heritable breast cancer cases and 80% of combined breast and ovarian cancer cases occur due to mutations in *BRCA1* (Yarden & Papa, 2006). More than 90% of the identified germ-line *BRCA1* mutations introduce premature termination codons into the *BRCA1* coding sequence; most of the truncated *BRCA1* mRNA transcripts are degraded by the nonsense-mediated mRNA decay pathway (Perrin-Vidoz, Sinilnikova, Stoppa-Lyonnet, Lenoir, & Mazoyer, 2002). Thus, the level of *BRCA1* truncated proteins expressed (if any) is very low.

Among sporadic cases of *BRCA1*-associated breast cancer, epigenetic silencing of *BRCA1* in the form of promoter hypermethylation rather than *BRCA1* mutations is commonly seen (Catteau & Morris, 2002). This results in the loss of *BRCA1* gene

expression. A few studies have also attributed the low expression of *BRCA1* in sporadic breast cancers to the degradation of BRCA1 proteins (Blagosklonny et al., 1999) and/or transcriptional repression of the *BRCA1* gene (Budhram-Mahadeo, Ndisang, Ward, Weber & Latchman, 1999).

BRCA1 and Base Excision DNA Repair

As mentioned previously (in the “Introduction” section of this thesis), several endogenous and exogenous factors are responsible for cellular oxidative stress. In addition to those factors, a breast-specific mechanism is also responsible for oxidative stress in breast tissues: the accumulation of hydrogen peroxide following the metabolism of 17β -estradiol by lactoperoxidase (Sipe, Jordan, Hanna, & Mason, 1994). Under these conditions, if the cellular antioxidant defense systems and/or DNA repair systems are compromised, the DNA begins to rapidly accumulate oxidative damage, resulting in genetic instability and initiation of breast carcinoma (Malins & Haimanot, 1991).

Previous studies in our laboratory (Alli, 2008) showed that mouse mammary epithelial cells deficient in *BRCA1* had higher levels of oxidative DNA damage (oxidized bases were measured using the comet assay) when compared to cells containing the wild-type *BRCA1*. In addition, *BRCA1*-mutated breast cancer cell lines (SUM149PT, SUM1315MO2, HCC1937, and MDAMB436) were found to be more sensitive to treatment with hydrogen peroxide when compared to normal (but immortalized) breast cell lines (MCF10A and MCF12A) (Alli, 2008). Since BER is the major pathway that repairs oxidative DNA damage, and a direct correlation between resistance to oxidative

DNA damage and cellular BRCA1 levels was seen in previous studies, we decided to investigate if BRCA1 was involved in the BER pathway.

In this study, we hypothesized that the BRCA1 protein plays a role in BER, and so breast tissue with low *BRCA1* expression or with a mutant *BRCA1* has defective BER, and thus increased oxidative DNA damage. This may then result in genetic instability leading to the initiation and progression of breast carcinogenesis. For our study, we used the SUM149PT breast cancer cell line. This is an adherent, ductal epithelial cell line that originated from the inflammatory breast carcinoma of a 35 year old patient (Elstrodt et al., 2006). The genome copy number aberrations and gene expression profile of this cell line has been previously studied (Neve et al., 2006). SUM149PT cells have a deletion (2288delT) in exon 11 of the *BRCA1* coding region, which results in a premature termination codon (Elstrodt et al., 2006) in the mRNA transcript. Semiquantitative RT-PCR analysis has previously confirmed the presence of very low levels (Elstrodt et al., 2006) or complete absence (Alli, 2008) of *BRCA1* mRNA transcripts in these cells, which could be due to the nonsense-mediated decay of the truncating transcripts. This is also consistent with previous results obtained following Western blot analysis (Alli, 2008; Elstrodt et al., 2006) and immuno-histochemistry (Elstrodt et al., 2006) on paraffin embedded cells, which showed the complete absence of BRCA1 proteins in the nucleus of SUM149PT cells. To test our hypothesis, a constitutive wild-type *BRCA1* expression plasmid was transfected into the SUM149PT cells. Cells transfected with the empty vector alone were used as a negative control. The transfected cells were then subjected to a novel host-cell reactivation assay (HCR) to measure in vivo BER activity.

Materials and Methods

Cell Lines and Media

SUM149PT cells (Asterand) were cultured in Ham's F12 media (Gibco) supplemented with 10% (vol/vol) fetal bovine serum (FBS) (Gibco), 1X penicillin/streptomycin/fungizone (P/S/F) (Mediatech Inc.), 5 µg/ml insulin (Sigma Aldrich), 1 µg/ml hydrocortisone (Sigma Aldrich) and 10 mM HEPES (Gibco). Their morphology, growth rate, and lack of *BRCA1* gene expression was regularly monitored in our laboratory (using RT-PCR and Western blotting). The earliest passages of the cell line were used for our experiments. MCF7 cells were cultured in media containing DMEM (Mediatech Inc), 10% FBS and 1X P/S/F. All the cells were maintained in 5% CO₂ at 37 °C. The cells were frozen in media containing 10% (vol/vol) DMSO.

Confirmation of the Wild-Type BRCA1 Construct and the Empty Vector Control

The wild-type *BRCA1* expression plasmid (pcDNA3β-*BRCA1*) and the empty vector control (pcDNA3) were kindly provided by Dr. Simon Powell (Washington University, St. Louis). The constructs were transformed into the OneShot[®] TOP10 chemically competent *E.coli* cells (Invitrogen) according to the manufacturer's instructions. Each transformation mix was then plated on LB agar plates containing 100 µg/ml ampicillin (Sigma Aldrich), and the plates were inverted, and incubated at 37 °C overnight. Single, well-isolated colonies were picked and grown overnight in sterile snap-capped polystyrene tubes containing 3 ml of LB/ampicillin (100 µg/ml) media at 37 °C, 250 rpm. Plasmids were isolated from 2 ml of each cell suspension using the

GenElute™ Plasmid Miniprep Kit (Sigma Aldrich), and their DNA concentration was estimated using UV-Vis spectrophotometry (BioPhotometer, Eppendorf). The remaining cell suspension was stored at 4 °C to prepare frozen glycerol stocks, once the positive clones were identified following restriction analysis.

If restriction analysis was not performed on the same day that the plasmids were isolated, then prior to plasmid isolation, cell suspensions from each sample were spotted on a grid-plate containing LB agar with 100 µg/ml ampicillin, and labeled. The plates were sealed and stored at 4 °C. Following identification of positive clones, cell suspensions were prepared from the corresponding grids as described before.

For the restriction analysis of the pcDNA3β-*BRCA1* construct, unique restriction sites on the pcDNA3 vector backbone (Invitrogen) and the *BRCA1* coding sequence (Genbank accession number NM_007294) were identified using Webcutter 2.0 (developed by Heiman, 1997). Two restriction sites (*NheI*, *XhoI*) on the pcDNA3β-*BRCA1* construct which on cutting would yield restriction fragments of unequal sizes, that would be easily detectable following gel analysis, were chosen. The pcDNA3 constructs were digested using the restriction enzyme *PstI*, as suggested by the manufacturer.

Plasmids (2.5 µg) isolated from the pcDNA3β-*BRCA1* transformed clones were digested at 37 °C for 2 hr with *NheI* (30 U) (Gibco BRL) in React 4 buffer (Gibco BRL), followed by digestion at 37 °C for 1 hr with *XhoI* (20 U) (NEB) in NEB 2 buffer (NEB). Plasmids obtained from pcDNA3 transformed clones were digested with *PstI* (30 U) (NEB) at 37 °C for 3 hr. A final concentration of 100 µg/ml of bovine serum albumin

(BSA) (NEB) was included in the *Pst*I restriction digest. The restricted plasmids were electrophoresed on a 1% agarose gel (containing 3 µg of ethidium bromide per ml of molten agarose) in Tris acetate EDTA (TAE) buffer, along with a 1 kb DNA ladder (Invitrogen). The DNA fragments on the gel were visualized using 300 nm UV illumination (ChemImager 4400, Alpha Innotech).

Large Scale Amplification of the Wild-Type BRCA1 Construct and Empty Vector Control for Use in Transfection

Prior to transfection, a small amount of frozen culture from the pcDNA3β-*BRCA1* and pcDNA3 glycerol stocks was removed and streaked on LB agar plates with 100 µg/ml ampicillin and incubated overnight at 37 °C. A single colony was removed and suspended in sterile snap-cap polystyrene tubes containing 2 ml of LB/ampicillin media (100 µg/ml) to prepare starter cultures. The tubes were then incubated at 37 °C, 250 rpm, for 8 hr. The starter cultures were then diluted 1/1000 into 100 ml of LB/ampicillin media (100 µg/ml) in a 500 ml flask and incubated overnight at 37 °C, 250 rpm. The plasmids were then isolated using HiSpeed Plasmid Maxi Kit (Qiagen) according to manufacturer's instructions, and quantified using UV-Vis spectrophotometry. The plasmid DNA was then stored at -20 °C until transfection.

Transient Transfection of the Wild-Type BRCA1 Construct and Empty Vector Control into SUM149PT Cells

The day before transfection, SUM149PT cells were plated at approximately 100 cells/cm² growth area of a T-25 tissue culture flask using regular growth media. Prior to transfection, cells were washed once with 1X phosphate-buffered saline (PBS) and replenished with 2 ml of Opti-MEM[®] I Reduced Serum Medium (Invitrogen). The pcDNA3 β -BRCA1 (10 μ g) and pcDNA3 (10 μ g) plasmids were transfected into the SUM149PT cells using Lipofectamine[™] 2000 (10 μ l) (Invitrogen), according to the manufacturer's instructions. A cell control that was treated only with Lipofectamine[™] 2000 (10 μ l) was included to monitor cytotoxicity from the transfection reagent. The cells were incubated at 37 °C in a CO₂ incubator for 24 hr (the media in the flasks was replaced with regular growth media 6 hr after transfection).

Nuclear Protein Extraction and Quantification

The SUM149PT cells were collected into microfuge tubes 24 hr following transfection, by scraping using a rubber policeman. The cells were pelleted by centrifugation at 1500 rpm for 5 min, and washed once with ice-cold 1X PBS. Nuclear proteins from these cells were extracted using the NE-PER[®] Nuclear and Cytoplasmic Extraction Reagents Kit (Pierce), according to the manufacturer's instructions. A protease inhibitor cocktail (Sigma Aldrich P8340) was added to the reagents specified by the manufacturer. The concentration of nuclear proteins extracted was then determined using the Bio-Rad Protein Assay (Biorad), according to the manufacturer's instructions

for the microtiter plate format. BSA was used as the standard, and the absorbance at 595 nm was measured using a microplate reader (Molecular Devices, Inc.).

Western Blot Analysis

The nuclear proteins (20 μ g) were denatured by boiling for 5 min in Laemmli Sample Buffer (Biorad), and resolved at 100 V on a Ready Gel Tris-HCl gradient gel (4-15%) (Biorad) using 1X Tris-glycine-SDS Buffer (Biorad). The Kaleidoscope Prestained Standards (Biorad) were included as molecular weight markers. Following electrophoresis, the gel was equilibrated in 1X Tris-glycine Buffer (Biorad) containing 20% (vol/vol) methanol. The proteins were then blotted overnight at 4 °C, onto a polyvinylidene fluoride (PVDF) membrane (Amersham Biosciences) using the Mini-Protein 3 transfer system (Biorad) (20 V), according to the manufacturer's instructions. Following transfer, the membrane was removed from the transfer system, oriented and blocked using 5% (wt/vol) milk for 1 hr at room temperature. Following a brief wash in phosphate-buffered saline containing 0.05% (vol/vol) Tween-20 (PBST), the entire membrane was cut horizontally, between the 130 kDa and 87 kDa molecular weight markers (identified by the colors of the markers). The portion of the membrane containing the 130 kDa and 205 kDa markers were probed overnight at 4 °C with anti-BRCA1 monoclonal antibody (2 μ g/ml) (Calbiochem) in 1% (wt/vol) milk and PBST. The other portion of the membrane containing markers between the molecular weights 7 kDa to 87 kDa, were probed for the TATA-binding protein (TBP) (a nuclear loading control) using anti-TBP monoclonal antibody (1/2000) (Abcam) in 1% (wt/vol)

milk and PBST. Following a brief wash, the two portions of the membrane were incubated in ECL[™] peroxidase labeled anti-mouse antibody (1/5000) (Amersham Biosciences), 3% (wt/vol) milk and PBST for 1 hr at room temperature. The membrane was then rinsed three times in PBST, treated with ECL[™] Western Blotting Detection Reagents (Amersham Biosciences) according to the manufacturer's instructions, and exposed on a HyperFilm ECL[™] (Amersham Biosciences). The film was processed (Konica SRX-101A Film Processor) following a 20 min exposure for BRCA1 and 1 min exposure for TBP.

Use of the Host-Cell Reactivation (HCR) Assay to Measure BER in SUM149PT Cells Transiently Transfected with Wild-Type BRCA1 or Empty Vector Constructs

Overview of the HCR assay for BER. The HCR assay to measure BER of 8oxodG lesions was developed by Dr. Elizabeth Alli (Ford laboratory, Stanford University). This assay uses recombinant adenovirus carrying a reporter gene coding for GFP (Ad-GFP). Photodynamic treatment (PDT) of DNA, which involves treatment of DNA with a photosensitizing dye and exposure to visible light, has previously been shown to introduce 8oxodG lesions (Schneider, Price, Maidt, Gutteridge, & Floyd, 1990). PDT of adenoviral virions using methylene blue (as a photosensitizer) and visible light has been shown to specifically induce damage to the DNA with little effect on the viral capsid (Schagen et al., 1999). In the HCR assay, the Ad-GFP virions are subjected to PDT to induce the formation of transcription-blocking 8oxodG lesions on the GFP reporter gene.

The damaged GFP reporter gene is then introduced into cells of interest via adenovirus-mediated gene transfer, and allowed sufficient time for repair. If the 8oxodG lesions on the GFP reporter gene are successfully repaired by the cellular BER pathway, the gene undergoes host-cell reactivation, and GFP is expressed. Thus, expression of GFP (detected using a fluorescence plate reader) indicates successful repair, whereas lack of GFP indicates compromised repair (Figure 3).

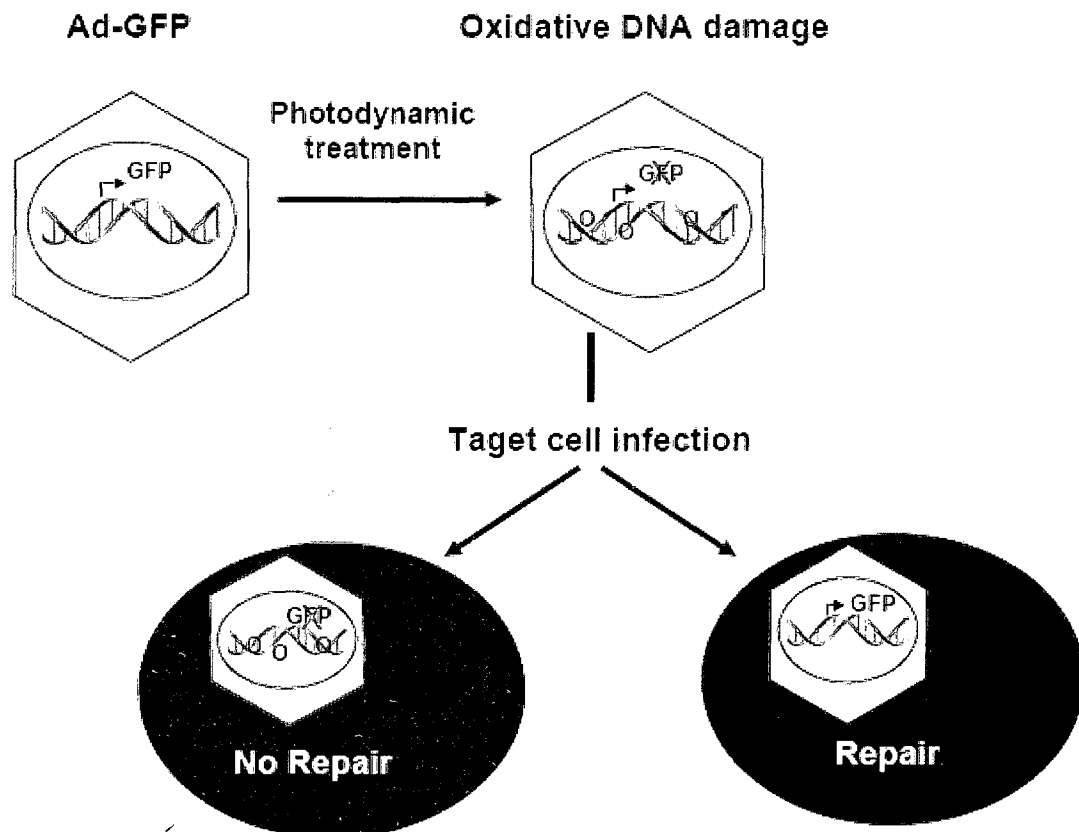


Figure 3. Overview of the host-cell reactivation assay to measure BER of 8oxodG lesions. Recombinant adenoviruses containing a GFP reporter gene (Ad-GFP) are subjected to photodynamic treatment (methylene blue and visible light) which induces 8oxodG lesions (O) on the GFP reporter gene, thus preventing its expression. Following

infection of the target cells, if cellular BER is efficient, the lesions are repaired and GFP is expressed. However, if cellular BER is compromised, the lesions are not repaired and no GFP is expressed. Reproduced with permission from the author (Alli, 2006).

Transient transfection of the wild-type BRCA1 and empty vector constructs into SUM149PT cells for the HCR assay. SUM149PT cells were plated 24 hr before transfection on nine wells (2×10^5 cells/well) of a 24-well plate. Three wells were transfected with the pcDNA3 empty vector control (1 μ g/well) and labeled “Vector Control”. The next three wells were transfected with the pcDNA3 β -*BRCA1* expression vector (1 μ g/well) and were labeled “BRCA1 WT”. The last three wells were left untransfected and were labeled “Cell Control” (Table 1). The transfections were performed using Lipofectamine TM 2000 (1 μ l/well) (Invitrogen), according to the manufacturer’s instructions. After 6 hr of incubation at 37 °C with 5% CO₂, the cells were replenished with 300 μ l of regular growth media and further incubated for 10-15 hr, to allow expression of the wild-type *BRCA1*.

Table 1

Designation of wells for the plating, transfection and infection of SUM149PT cells in the HCR assay

| Position of well (24-well plate) | Designation of well |
|----------------------------------|------------------------------|
| A1 | Vector control – “Count” |
| B1 | Vector control – “Undamaged” |
| C1 | Vector control – “Damaged” |
| A2 | BRCA1 WT - “Count” |
| B2 | BRCA1 WT - “Undamaged” |
| C2 | BRCA1 WT - “Damaged” |
| A3 | Cell control - “Count” |
| B3 | Cell control - “Undamaged” |
| C3 | Cell control - “Damaged” |

Note. Vector control = SUM149PT cells transfected with pcDNA3 empty vector; BRCA1 WT = SUM149PT cells transfected with pcDNA3 β -BRCA1 expression vector; Cell control = untransfected SUM149PT cells; Count = well of cells that was trypsinized and counted; Undamaged = well of cells infected with the undamaged Ad-GFP viruses (exposed to only the photosensitizer); Damaged = well of cells infected with the damaged Ad-GFP viruses (exposed to both the photosensitizer and visible light).

PDT and adenoviral infection. One well of cells (labeled “Count”) from each of the three sets of wells labeled “Vector control”, “BRCA1 WT” and “Cell control” (Table 1) was trypsinized, and the cells were counted using a hemacytometer. SUM149PT cells are typically infected with 50 pfu of adenovirus per cell. The number of cells counted per

well was then used to estimate the total volume of Ad-GFP virions required for infection. While one batch of the Ad-GFP virions (labeled “Damaged”) was subjected to PDT (i.e., treatment with 0.5 μ M methylene blue and exposure to 2 mW/cm² visible light) for 1 min, another batch (labeled “Undamaged”) was treated only with 0.5 μ M methylene blue but not exposed to visible light. The PDT was carried out in the dark. In order to reduce heat damage to the virus, the PDT was performed on ice and a dish of sterile water was used between the light source and the plate containing the virus, to absorb heat. The cells in the wells labeled “Damaged” and “Undamaged” (Table 1) were then infected with the damaged virus (50 pfu/cell) and undamaged virus (50 pfu/cell) respectively. The infection was carried out in the dark. The infected cells were then incubated at 37 °C with 5% CO₂ for 24 hr (the cells were washed with 1X PBS and replenished with regular growth media 4 hr after infection).

HCR analysis. The cells were washed 24 hr following infection, trypsinized, and resuspended in regular growth media. The cells were centrifuged at 1500 rpm for 5 min, washed once with 1X PBS, and resuspended in 500 μ l of 1X PBS. The cells were then counted and the cell suspensions were normalized to the sample containing the lowest cell number, in a final volume of 500 μ l of 1X PBS. Each sample (100 μ l) was aliquoted in quadruplicates on to a black 96-well plate. Wells containing only 1X PBS were used to record background fluorescence. GFP expression was measured using a fluorescence plate reader (Flexstation II-384, Molecular Devices Inc.), and calculated as a ratio of the

fluorescence readings from cells infected with the damaged virus to those infected with the undamaged virus.

Results

Confirmation of the Wild-Type BRCA1 Construct and the Empty Vector Control

Prior to use in the transfection of SUM149PT cells, the pcDNA3 β -*BRCA1* and the pcDNA3 constructs that were kindly provided by Dr. Simon Powell were confirmed by DNA restriction analysis. While the restriction enzyme to use (*Pst*I) for the analysis of the pcDNA3 vector was specified by the manufacturer (Invitrogen), the enzymes to use for the confirmation of the pcDNA3 β -*BRCA1* construct were unknown. Thus, the Webcutter 2.0 program was used to generate a list of restriction enzymes that uniquely cut the *BRCA1* coding sequence and the pcDNA3 vector backbone in the pcDNA3 β -*BRCA1* construct. From this list, *Nhe*I (uniquely cuts the *BRCA1* coding sequence) and *Xho*I (uniquely cuts the vector backbone) enzymes were chosen, because these enzymes when used to cut the pcDNA3 β -*BRCA1* construct will generate two fragments of unequal sizes (1940 bp and 9766 bp) that can be easily visualized on an agarose gel.

Following restriction analysis of the plasmids isolated from the pcDNA3 β -*BRCA1* and the pcDNA3 transformed bacterial clones, the products of restriction were run on a 1% TAE-agarose gel (Figure 4). All the clones tested were found to be positive for the respective vectors. The plasmids isolated from the clones transformed with the pcDNA3 vector, following digestion with *Pst*I (lanes 3 to 6), gave two bands of expected sizes (1385 bp and 4061 bp) as specified by the manufacturer. Following digestion with *Nhe*I

and *XhoI*, the plasmids isolated from the clones transformed with the wild-type *BRCA1* construct (lanes 7 and 8) gave two bands of the expected sizes (1940 bp and 9766 bp).

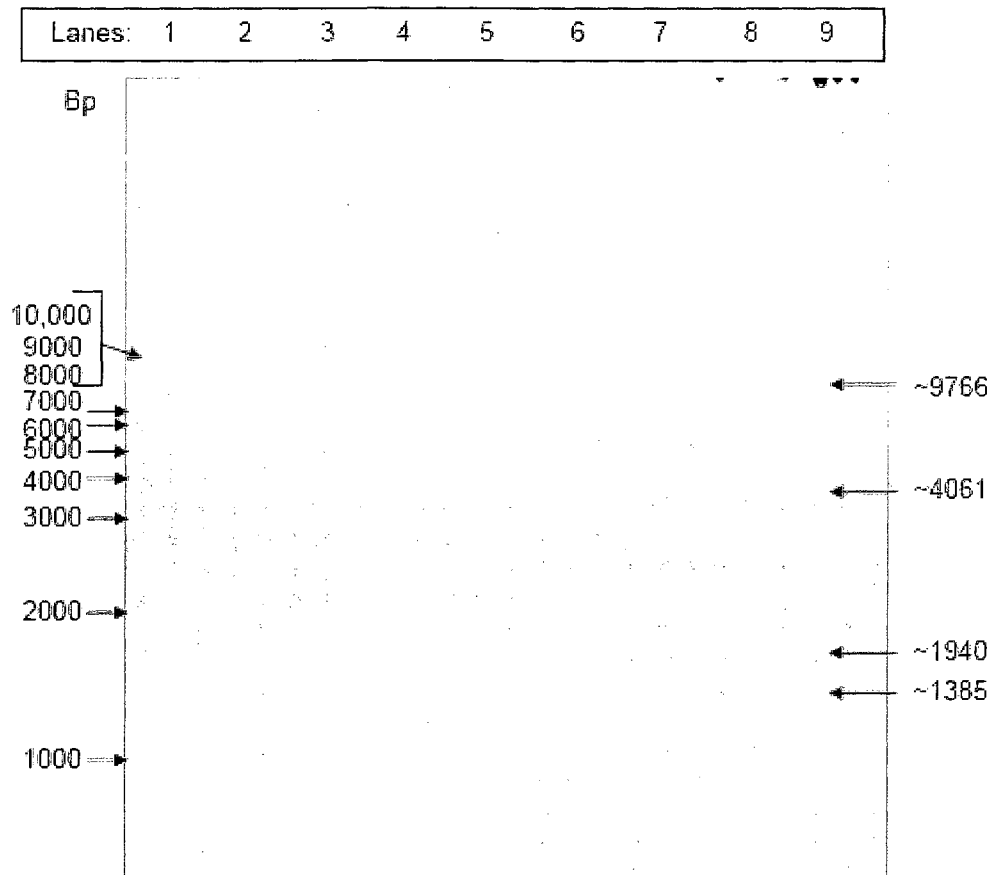


Figure 4. Restriction analysis of the plasmids isolated from bacterial clones transformed with the wild-type *BRCA1* or the pcDNA3 constructs. Plasmids isolated from bacterial clones following transformation with the wild-type *BRCA1* and pcDNA3 constructs were digested with *NheI/XhoI* and *PstI* respectively, and electrophoresed on a 1% TAE-agarose gel (stained with ethidium bromide). Lanes 1, 9 = empty; lane 2 = 1 kb DNA ladder; lanes 3,4,5,6 = *PstI* restricted plasmids from pcDNA3 transformed clones; lanes 7, 8= *NheI/XhoI* restricted plasmids from pcDNA3 β -*BRCA1* transformed clones. Bp = base pair.

Confirmation of Wild-Type BRCA1 Expression in SUM149PT Cells Transfected with the pcDNA3 β -BRCA1 Expression Vector

Prior to analysis of the nuclear extracts from SUM149PT cells transfected with wild-type *BRCA1*, nuclear extracts from a positive control cell line (MCF7) was analyzed by Western blotting using the anti-BRCA1 monoclonal antibody. The antibody was found to specifically recognize the 220 kDa BRCA1 protein (Figure 5A). In our study, transfection of the SUM149PT cells with the empty pcDNA3 vector showed no BRCA1 protein expression, whereas transfection of the pcDNA3 β -*BRCA1* construct into these cells showed the presence of BRCA1 proteins in the nucleus (Figure 5B).

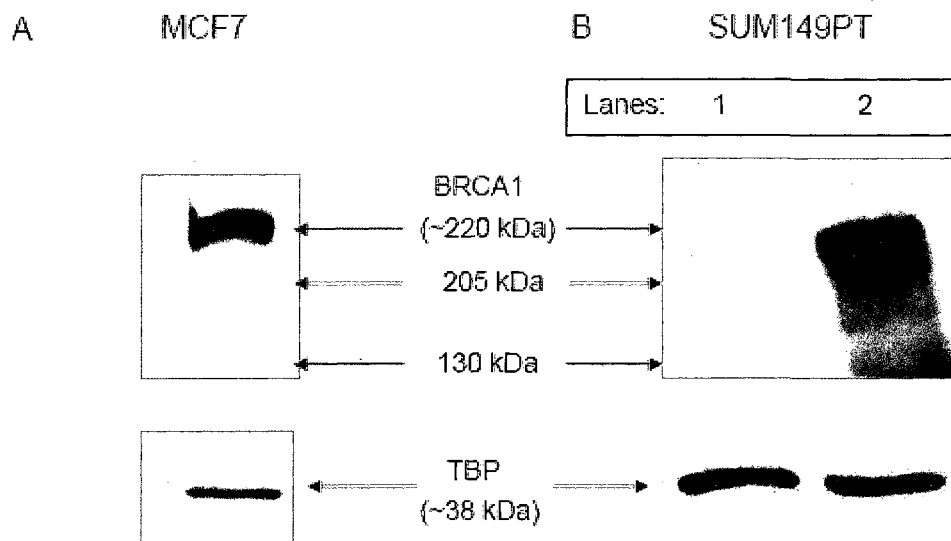


Figure 5. Western blot analysis of nuclear extracts from MCF7 cells and SUM149PT cells transfected with wild-type *BRCA1* or the empty vector constructs. Nuclear extracts from MCF7 cells (A) were collected, subjected to SDS-PAGE gel electrophoresis using a 4-15% gradient Tris-HCl gel. The proteins were blotted onto a PVDF membrane and the membrane was probed using anti-BRCA1 monoclonal antibody and ECLTM peroxidase

labeled anti-mouse antibody. TATA-binding protein (TBP) was used as a nuclear loading control. Nuclear extracts from SUM149PT cells (B) transfected with either the empty pcDNA3 vector (lane 1) or the wild-type *BRCA1* construct (lane 2) were analyzed as described for the MCF7 cells. kDa = kilo Dalton.

BER Activity in SUM149PT Cells Transiently Transfected with Wild-Type BRCA1 and Empty Vector Control

The HCR assay was performed to detect the efficiency of BER in SUM149PT cells transiently transfected with the wild-type *BRCA1* and the empty vector constructs. The green fluorescence from GFP expression was recorded in wells containing an *equal number* of transfected (with pcDNA3 or *BRCA1* constructs) SUM149PT cells that were infected either with the undamaged or damaged Ad-GFP virus. The relative GFP expression in the *BRCA1* wild-type or empty vector transfected SUM149PT cells was then calculated as a ratio of the fluorescence readings obtained from cells infected with the damaged virus to those infected with the undamaged virus (Figure 6). An approximately two-fold increase in relative GFP expression in cells transfected with the wild type *BRCA1* expression vector, when compared to those transfected with the empty pcDNA3 vector was observed. Untransfected SUM149PT cells subjected to the HCR assay showed similar relative GFP expression (0.6) when compared to that of cells transfected with the pcDNA3 vector (0.5). This shows that the vector backbone in the wild-type *BRCA1* construct did not enhance BER activity.

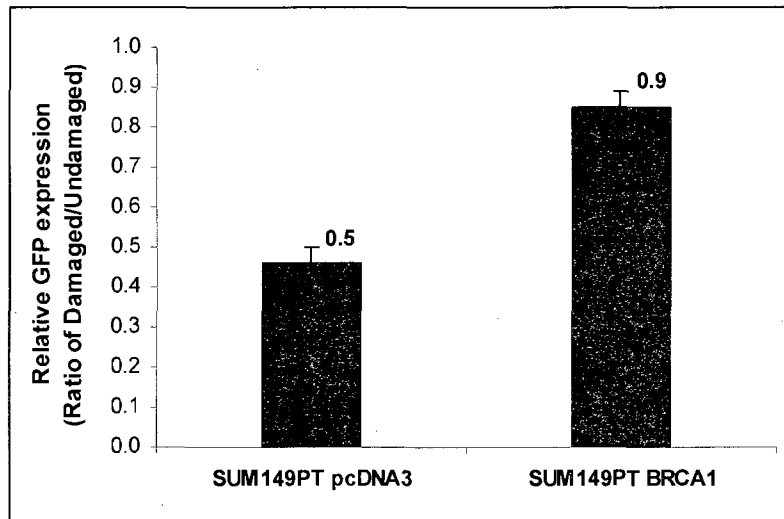


Figure 6. Relative GFP expression from the HCR assay to measure BER in SUM149PT cells transfected with wild-type *BRCA1* or empty vector constructs. SUM149PT cells transiently transfected with either the empty vector control (SUM149PT pcDNA3) or the wild-type *BRCA1* expression vector (SUM149PT *BRCA1*) were subjected to the HCR assay to measure BER as described in the Methods section. The green fluorescence was recorded in quadruplicate wells (for each cell type) containing an equal number of cells, using a fluorescence plate reader. The relative GFP expression for each cell type was calculated as a ratio of the average fluorescence obtained for cells infected with the damaged virus to that of the undamaged virus. Each bar represents the average of the relative GFP expression for each cell type from two independent experiments. Vertical lines represent standard errors of the means.

A few modifications to the assay methodology was later made (Alli, 2008), which included the use of the same cell numbers for measuring GFP expression in each experiment, in order to compare results obtained from different experiments. Using these modifications, when the assay was later repeated several times (Alli, 2008), an approximately four-fold increase in relative GFP expression from cells transfected with the wild-type *BRCA1* construct when compared to those transfected with the empty vector control, was observed.

Discussion

BRCA1 has been known as a “caretaker” of the genome (Kinzler & Vogelstein, 1997) due to its role in multiple cellular processes that maintain genomic integrity. It has been implicated in the HR and NHEJ pathways to repair DNA double-stranded breaks (Zhang & Powell, 2005; Zhuang et al., 2006), and in the transcription-coupled repair (TCR) (Wang et al., 2000) and global genomic repair (GGR) (Hartman & Ford, 2002) sub-pathways of NER. However, the role of BRCA1 in the BER pathway was unknown.

A direct correlation between cellular levels of BRCA1 and resistance to oxidative stress has previously been reported in prostate cancer cells (DU-145) (Bae et al., 2004) and in mouse mammary epithelial cells (Alli, 2008). BRCA1 was found to up-regulate the expression of antioxidant genes in the study conducted by Bae et al. (2004). Although this may explain the BRCA1-mediated resistance to oxidative stress, we wanted to investigate if BRCA1 was involved in the BER pathway.

A breast cancer cell line (SUM149PT) known to contain a *BRCA1* truncation mutation (2288delT) that resulted in an absence of BRCA1 protein expression was chosen for our study. A wild-type *BRCA1* expression vector and the empty vector (lacking the *BRCA1* coding sequence) were confirmed by restriction analysis prior to their transfection into SUM149PT cells. These plasmids were previously sequenced and were found to contain no mutations (Scully et al., 1996). Due to the large size of the *BRCA1* expression plasmid (which would require the use of multiple primers), we did not re-sequence the plasmid following restriction analysis. However, following transfection

of SUM149PT cells with the wild-type BRCA1 construct, we detected (by Western blotting) the presence of full-length BRCA1 proteins in the nucleus. This also suggests that the BRCA1 proteins were functional, since truncated BRCA1 proteins have been shown to be unable to translocate into the nucleus to form nuclear foci and function in DNA damage response (Scully et al., 1999). The SUM149PT cells transfected with the wild-type *BRCA1* expression vector or the empty vector were subjected to the HCR assay to monitor in vivo BER activity. Results from our study suggested that SUM149PT cells expressing wild-type BRCA1 proteins have enhanced BER activity.

BRCA1 may enhance BER activity through transcriptional regulation or direct/indirect interactions with the proteins involved in the pathway. An immunoprecipitated BRCA1 protein complex containing USF2, a transcription factor, has been shown to specifically bind a novel consensus DNA sequence (TTC(G/T)GTTG) (Cable et al., 2003). Screening of the regulatory regions of genes directly or indirectly involved in BER for this consensus DNA sequence, may enable identification of BER genes (if any) that are transcriptionally regulated by BRCA1. BRCA1 has been shown to interact with components of the basal transcriptional machinery such as RNA polymerase II holoenzyme and histone deacetylases (Lane, 2004; Monteiro, 2000). Thus, it may nonspecifically regulate transcription of BER related genes. BRCA1 may also facilitate the access of BER proteins to the oxidized bases through its association with the chromatin remodeling proteins SW1 and SNF (Bochar et al., 2000).

The tumor suppressor p53 has been shown to enhance the hOGG1- and APE1-mediated cleavage steps in the BER pathway (Achanta & Huang, 2004). BRCA1,

through its interaction with p53 (Zhang et al., 1998), may indirectly regulate BER activity. On the other hand, BRCA1 may interact directly with the proteins involved in BER through its BRCT domain. This domain, found in the carboxyl terminal end of the BRCA1 protein, is often found in other proteins involved in DNA repair and maintenance of genomic stability (Yarden & Papa, 2006). Such proteins have the ability to form homo- and heterodimers through the interaction of their BRCT domains (Caldecott, 2003). The XRCC and Ligase III proteins involved in BER have been shown to heterodimerize through their BRCT domains (Dulic et al., 2001). It is likely that heterodimerization of the BRCA1 protein with either of these proteins could enhance their activity in the BER pathway.

In conclusion, preliminary investigations in our study have shown that BRCA1 enhances the BER pathway. These results will have to be confirmed using another assay for BER. Although it has been shown that immortalized cell lines retain many of the characteristics of the primary tissue (Neve et al., 2006), upon long-term culture, they may acquire new mutations in vitro. Thus, in the future, it may be useful to monitor BER in *BRCA1*-mutated primary breast cancer cells, before and after transfection with a *BRCA1* expression vector. Besides the up-regulation of antioxidant genes, the putative involvement of BRCA1 in the BER pathway suggests yet another mechanism by which the tumor suppressor may resist oxidative DNA damage in mammary tissue. The lack of these critical functions may explain the increased susceptibility to oxidative DNA damage previously observed in *BRCA1*-mutated breast cancer cells. Future research on

the precise role of BRCA1 in the BER pathway may facilitate the development of improved therapeutic strategies for BRCA1-associated breast and ovarian cancers.

CHAPTER TWO

DEVELOPMENT OF A NOVEL ASSAY TO MEASURE IN VIVO BER

Introduction

The 8oxodG lesions are one of the most frequently observed oxidation products (Poulsen, Prieme, & Loft, 1998) and have been commonly used as indicators of cellular oxidative stress. These lesions are excised by the hOGG1 DNA glycosylase (Rosenquist, Zharkov, & Grollman, 1997) and repaired primarily using the BER pathway (Lindahl, 1993). The efficiency of cellular BER of 8oxodG lesions may be measured using one of two methods. The first method involves monitoring the disappearance of 8oxodG lesions with time, on genomic DNA, following induction of cellular oxidative stress. The second method involves monitoring the disappearance of 8oxodG lesions on a DNA repair substrate either in vitro or in vivo.

Nonsubstrate Based Methods to Measure BER

Some of the techniques available to measure BER do not use DNA repair substrates. Instead, they measure BER of 8oxodG lesions by monitoring the disappearance of the lesions on cellular genomic DNA, following exposure of the cells to oxidizing agents. High performance liquid chromatography with electrochemical detection (HPLC-ECD) has been used to measure 8oxodG bases on genomic DNA,

following digestion of DNA using nuclease P1 and alkaline phosphatase (Anson, Hudson, & Bohr, 2000; Degan et al., 1995; Floyd, Watson, Wong, Altmiller, & Rickard, 1986). This method is expensive, requires a large sample volume and is capable of generating artifacts during sample preparation and chromatography (Ravanat et al., 2002). A common enzymatic method used to measure cellular 8oxodG levels following induction of oxidative stress involves the conversion of the 8oxodG lesions into DNA strand breaks using formamidopyrimidine DNA glycosylase. The breaks are subsequently detected using the comet assay (reviewed by McKelvey-Martin, Green, Schmezer, Pool-Zoberl, & Collins, 1993). This assay is inexpensive, requires very small amounts of DNA, and enables detection of heterogeneity in a cell population by measuring damage in single cells (Collins, Cadet, Moller, Poulsen, & Vina, 2004). However, this assay may sometimes underestimate 8oxodG levels due to inaccessibility of the lesions to the enzyme (occurs when the lesions are present in DNA loops) and due to the insensitivity of the assay above a certain level of DNA breakage (occurs when the tail end of the comet is saturated) (Collins & Dušinská, 2002; Collins et al., 2008). In addition, the assay is difficult to reproduce and requires careful optimization of experimental conditions to avoid detection of nonspecific strand breakage.

Other assays use fluorescein isothiocyanate (FITC) conjugated 8oxodG binding proteins to detect cellular 8oxodG lesions by fluorescence microscopy or flow cytometry, following exposure of cells to oxidizing agents. Although simple and inexpensive, these methods suffer from high levels of background fluorescence due to either nonspecific binding of the FITC-conjugated proteins, or high basal levels of endogenous 8oxodG

lesions which occur as a result of cellular metabolism. As a result, the assay is not sensitive enough to detect differences in 8oxodG levels before and after treatment with oxidizing agents (unpublished observations, Ford laboratory).

Immunoaffinity based methods for the detection and quantification of 8oxodG lesions have been previously described (Degan, Shigenaga, Park, Alperin, & Ames, 1991; Musarrat & Wani, 1994; Yin et al., 1995). An immunoaffinity-chromatography based 8oxodG ELISA using monoclonal antibodies (Yin et al., 1995) showed results comparable to those obtained using HPLC. Depending on the specificity of the antibody used, ELISA is a convenient, sensitive and relatively inexpensive assay to quantify 8oxodG lesions. A number of commercial 8oxodG ELISA kits (Trevigen Inc., Japan Institute for the Control of Aging, Genox Corp.) have recently been developed to measure 8oxodG levels in urine and serum samples. However, besides 8oxodG lesions, these kits can also detect and quantify RNA-based guanine oxidation products. If these kits were to be used with genomic DNA, they would then not only measure 8oxodG levels on the DNA, but also measure guanosine or its oxidation products (such as 8-bromoguanosine, 8-mercaptoguanosine, and N2-methylguanosine, etc.) on any contaminating RNA. Thus, when used with genomic DNA, these kits may not reliably indicate the efficiency of cellular BER of 8oxodG lesions.

Substrate Based Methods to Measure BER

In vitro studies using cell extracts and plasmid DNA substrates have greatly advanced our understanding of the enzymology and steps involved in the repair of

8oxodG lesions (Dianov, Bischoff, Piotrowski, & Bohr, 1998; Fortini et al., 1999; Hazra, Izumi, Maidt, Floyd, & Mitra, 1998). However, one study (Cappelli, Degan, & Frosina, 2000) reported the poor repair of 8oxodG lesions in vitro, using cell extracts from human fibroblast GM5757. In vitro BER may not be an accurate model of in vivo repair due to potential modifications of physiological conditions, disruption of repair protein complexes, interference from reagents in cell lysis buffers, and inconsistencies in the performance of cell extracts. In addition, the use of radiolabeled reagents in most of the in vitro assays further imposes cost and safety limitations.

The HCR assay described in chapter one is an in vivo (cell-based) BER assay, that monitors the repair of 8oxodG lesions on the GFP-coding region of recombinant adenoviruses (Ad-GFP). Although it measures repair in vivo, it is an end-point assay; the repair of 8oxodG lesions is measured by the expression of functional GFP 24 hr after infection. Thus, the HCR assay cannot obtain steady-state measurements of in vivo BER.

In this study, we have designed a novel assay to measure the in vivo BER of 8oxodG lesions using a biotin-tagged oligonucleotide DNA substrate, containing a single 8oxodG lesion on the untagged DNA strand (target strand). Briefly, the assay involves the transfection of the biotin-tagged substrate DNA into target cells and incubation for an increasing period of time to allow repair of the 8oxodG lesions. The cells are then lysed and the biotin-tagged substrate DNA is captured on streptavidin-coated beads and denatured, to isolate the untagged target DNA strand from the biotin-tagged complementary DNA strand. The 8oxodG lesions on the target DNA strands are then measured using the HT 8oxodG competitive ELISA Kit (Trevigen Inc.). The amount of

lesions detected on the target DNA is inversely proportional to the efficiency of cellular BER. When used with the tagged substrate DNA in this assay, the 8oxodG ELISA may provide a more reliable estimate of the efficiency of cellular 8oxodG BER when compared to its use with genomic DNA, because the tagged substrate DNA can be captured and purified from any contaminating DNA or RNA.

This chapter describes the design of this novel assay for measuring BER of 8oxodG lesions and optimization of the experimental conditions for some of the steps in the assay. The optimal working conditions for the assay were determined from the last step of the assay to the first, and each section of this chapter has been written in the same order. That is, the optimization experiments were performed first for the ELISA step of the assay, followed by the binding of the biotin-tagged substrate DNA to the streptavidin-coated beads, its denaturation and quantification, and finally, the transfection of the substrate DNA into target cells. This order was chosen since knowledge of the minimal amount of DNA required for the ELISA would enable an estimation of the amount of DNA to be used for titration of the streptavidin-coated beads, and ultimately for transfection.

In the future, following validation of the assay *in vivo*, it may be used to identify potential cancer genes that regulate the BER pathway.

Materials and Methods

Single-Stranded DNA Oligonucleotides

The following oligonucleotide DNA strands were used to prepare the substrate and control DNA:

1. Biotinylated DNA strand (nontarget DNA strand) (Operon)

The nontarget DNA strand (28-mer) has a biotin-TEG tag at the 3' end and consists of the following sequence:

5'-GCAGCCCGGGGGATCCACTAGTTCTAAG-Bt-3' (where Bt represents Biotin).

2. +8oxodG DNA strand (target DNA strand) (Midland Certified Reagents)

The target DNA strand (24-mer) has a single 8oxodG lesion at position 10 (from the 5' end) and consists of the following sequence:

5'-GAACTAGTGOATCCCCCGGGCTGC-3' (where O represents 8oxodG)

3. -8oxodG DNA strand (control DNA strand) (Operon)

The control DNA strand (24-mer) is identical in nucleotide sequence to the target DNA strand, but with a guanine instead of the 8oxodG lesion at position 10. It has the following sequence: 5'-GAACTAGTGGATCCCCCGGGCTGC-3'.

Gel Analysis of the Single-Stranded DNA Oligonucleotides

The single-stranded +8oxodG, -8oxodG and biotinylated DNA oligonucleotides were resuspended in 1X Tris-EDTA (TE) buffer, aliquoted, and stored at -20 °C. The DNA oligonucleotides (50 ng) were then denatured by heating at 90 °C for 5 min in a

solution containing 95% (vol/vol) formamide, 30% (vol/vol) glycerol, 0.25% (wt/vol) bromophenol blue and 0.25% (wt/vol) xylene cyanol FF (Sambrook, Fritsch, & Maniatis, 1989). The denatured DNA samples were placed on ice until they were ready to load onto a 15% Tris-borate-EDTA (TBE)-polyacrylamide 7 M urea gel. The gel was prerun for 30 min at 110 V. The samples were then loaded and electrophoresed at 110 V for approximately 1 hr. A 10 bp DNA ladder (Integrated Technologies) was denatured as described for the samples, and included in the gel. The DNA bands were visualized using 300 nm UV illumination (ChemImager 4400, Alpha Innotech), following staining with SYBR[®] Green II (Invitrogen) according to the manufacturer's instructions. SYBR[®] Green II was used because it binds with higher affinity to single-stranded than double-stranded DNA (Invitrogen).

Preparation of the Substrate and Control DNA

Annealing. The substrate DNA (+ 8oxodG/biotinylated DNA) and the control DNA (- 8oxodG/biotinylated DNA) were prepared by annealing the single-stranded oligonucleotides as previously described (Achanta & Huang, 2004). Briefly, the +8oxodG or -8oxodG DNA strands (2 pmol/ μ l) and the biotinylated DNA strands (1 pmol/ μ l) were mixed in an annealing buffer consisting of a final concentration of 10 mM Tris-hydrochloride (Tris-HCl) (pH 7.5), 5 mM magnesium chloride, and 30 mM sodium chloride (NaCl). The solution was heated to 85 °C and allowed to gradually cool to room temperature. The annealed DNA was aliquoted and stored at -20 °C.

Quantification. The annealed substrate and control DNA were quantified by fluorimetry using SYBR[®] Green I (Invitrogen). The NoLimits[™] 25 bp DNA fragment (Fermentas) was used to generate a DNA standard curve ranging from 0-500 ng/ml. The SYBR[®] Green I dye was diluted (1/5000), and 500 µl of the diluted dye was added to 500 µl of diluted annealed DNA (1/100 or 1/1000), and the solution was mixed well. Following incubation at room temperature (in the dark) for 5 min, 200 µl aliquots of the solution were loaded in quadruplicate wells of a black 96-well plate. Fluorescence was recorded using a fluorescence plate reader (Flexstation II-384, Molecular Devices Inc.) at the excitation and emission wavelengths of 497 nm and 520 nm respectively.

Gel analysis. The annealed substrate and control DNA (25 ng) were mixed with 30% (vol/vol) glycerol, 0.25% (wt/vol) bromophenol blue and 0.25% (wt/vol) xylene cyanol FF (Sambrook et al., 1989), and electrophoresed at 110 V on a 15% nondenaturing TBE-polyacrylamide gel. The gel was stained using SYBR[®] Green I (Invitrogen) according to the manufacturer's instructions, and visualized using 300 nm UV illumination. A 10 bp DNA ladder (Invitrogen) was also included.

8oxodG Competitive ELISA

The reagents from the HT 8oxodG ELISA Kit (Trevigen), including the 8oxodG coated ELISA plate, the standards consisting of 8oxodG bases and the anti-8oxodG antibody, were used to quantify 8oxodG lesions in our BER assay. The ELISA was performed according to the manufacturer's instructions. Briefly, the 8oxodG standards

and the single-stranded +8oxodG or -8oxodG DNA (5 ng each) were added to triplicate wells (50 µl/well) of the 96-well plate precoated with 8oxodG lesions. Then, diluted anti-8oxodG monoclonal antibody (50µl/well) was added, the plate was covered, and incubated at 37 °C for 1 hr. Following incubation, the wells were washed six times with the 1X wash buffer provided (200µl/well). Diluted horseradish peroxidase (HRP) conjugated anti-mouse secondary antibody (100 µl/well) was then added; the plate was covered and incubated for 1 hr at 37 °C. The wells were then washed as described before. The 3,3',5,5' – tetramethylbenzidine (TMB) substrate (100 µl/well) was added to the wells and the plate was incubated in the dark for 15 min. The reaction was stopped using the stop solution provided (1 N hydrochloric acid) and the absorbance values at 450 nm was measured using a microplate reader (Molecular Devices Inc.). The intensity of the yellow color is inversely proportional to the concentration of 8oxodG in the sample or standard. The 8oxodG standard curve was used to determine the amount of 8oxodG lesions on the +8oxodG and -8oxodG DNA.

Titration of the Amount of Streptavidin-Coated Magnetic Beads to use in the BER Assay

The Dynabeads[®] M-270 Streptavidin (Invitrogen) were washed and prepared for binding according to the manufacturer's instructions. The double-stranded control DNA (100 ng) was mixed with the beads (10 µg, 50 µg, 100 µg, 150 µg) and incubated according to the manufacturer's instructions. Briefly, the DNA and the beads were mixed in a solution containing a final concentration of 5 mM Tris-HCl (pH 7.5), 0.5 mM EDTA and 1 M NaCl (1X Binding and Washing [B&W] buffer) and incubated at room

temperature for 15 min. The tube was tapped every 3 min to resuspend the beads. At the end of the incubation, the tubes were placed on a magnetic stand (Promega) for 2 min and the supernatant was removed and discarded. The beads were then washed twice in the 1X B&W buffer. The beads (containing the bound, double-stranded control DNA) were then resuspended in 25 μ l of 0.1 M sodium hydroxide (NaOH) to denature the double-stranded DNA into single-stranded -8oxodG and biotinylated DNA strands. The solution was incubated at room temperature for 5 min (on a shaker). The tube was then placed on a magnet for 2 min, after which the supernatant (containing the denatured, untagged -8oxodG DNA strands) was collected and stored at 4 °C. A small volume (5 μ l) of the supernatant eluted from each of the four experiments (10 μ g, 50 μ g, 100 μ g, 150 μ g beads) was electrophoresed on a 12% TBE-polyacrylamide 8.3 M urea gel as described before (“Gel analysis of the single-stranded oligonucleotides” section of this chapter). A fixed amount of the -8oxodG DNA strand (11 ng) was also electrophoresed to serve as a reference band of known concentration while estimating the amount of DNA in the sample lanes. A 10 bp DNA ladder (Integrated Technologies) was also included. The intensity of the DNA bands was determined using Image J software v1.37 (developed by Rasband, 2006).

Quantification of DNA

The single-stranded -8oxodG DNA was used to generate a standard curve ranging from 0-50 ng/ml (in 10 ng/ml increments). The fluorescent dyes SYBR[®] Green II (Invitrogen) and Quant-iT[™] Oligreen ssDNA Reagent (Invitrogen) were diluted

according to the manufacturer's instructions. The DNA standards (500 μ l) were mixed with either of the two diluted dyes (500 μ l), incubated at room temperature (in the dark) for 5 min, and aliquots (200 μ l) were loaded in quadruplicate wells of a black 96-well plate. The fluorescence was recorded using a fluorescence plate reader at the excitation/emission wavelengths of 497 nm/520 nm and 480 nm/520 nm for the SYBR[®] Green II and Quant-iT[™] Oligreen dyes respectively.

Cell Lines and Media

SUM149PT cells were cultured in Ham's F12 media supplemented with 10% (vol/vol) FBS, 1X P/S/F, 5 μ g/ml insulin, 1 μ g/ml hydrocortisone and 10 mM HEPES. MCF7 cells were cultured in media containing DMEM, 10% FBS and 1X P/S/F. All the cells were maintained in 5% CO₂ at 37 °C.

Selection of a Suitable Transfection Reagent

Transfection. SUM149PT cells were plated (1×10^5 cells per well) on a 24-well plate using 500 μ l of regular growth media, and allowed to adhere overnight. Double-stranded control DNA (800 ng) was transfected into each well using either Lipofectamine[™] 2000 (2 μ l/well) (Invitrogen) or Oligofectamine[™] (2 μ l/well) (Invitrogen) transfection reagent, according to the manufacturer's instructions. In order to monitor cell death from treatment with the transfection reagents, untransfected cell controls that were treated only with either of the two reagents were prepared. The cells were incubated for 4 hr at 37 °C in a CO₂ incubator.

Cell lysis, DNA capture, denaturation, and quantification following transfection.

Following transfection of the control DNA and incubation for 4 hr, the cells were trypsinized, quenched using regular growth media and centrifuged at 1500 rpm for 5 min. The cell pellet was washed once in 500 μ l of 1X PBS. The pellet was then resuspended in 20 μ l of cell lysis buffer (50 mM Tris-HCl (pH 7.4), 150 mM NaCl, 1 mM EDTA, 1 mM EGTA, and 1% Triton-X 100). Protease inhibitor cocktail (1X) (Sigma Aldrich P8340) was added to the lysis buffer prior to use. The cells were rotated at 4 °C for 1 hr and centrifuged at 14,000 rpm for 10 min (Hou, Prasad, Asagoshi, Masaoka, & Wilson, 2007). The supernatant was removed and stored at -20 °C until future use.

The Dynabeads[®] M-270 Streptavidin (Invitrogen) were washed and prepared for binding according to the manufacturer's instructions. The cell lysate was thawed on ice prior to use. The NaCl and EDTA concentrations in the lysate were adjusted prior to the addition of streptavidin-coated magnetic beads, to facilitate bead binding. The recommended bead binding conditions are 5 mM Tris HCl (pH 7.5), 0.5 mM EDTA, and 1 M NaCl (Invitrogen). The beads (850 μ g) were then added to the cell lysate, incubated to allow for DNA capture, and washed, according to the manufacturer's instructions. The DNA bound to the beads was then denatured using 0.1 M NaOH and the supernatant was collected as described before ("Bead titration" section of this chapter). The DNA recovered in the supernatant was then quantified using the Quant-iT[™] OliGreen[®] ssDNA reagent (Invitrogen), as described before ("DNA quantification" section of this chapter).

Transfection of Control and Substrate DNA into SUM149PT and MCF7 cells, DNA Capture and Denaturation

SUM149PT and MCF7 cells were plated as described before (“Selection of a transfection agent” section of this chapter). The cells were transfected with the double-stranded control DNA (800 ng) or the substrate DNA (800 ng), using Lipofectamine™ 2000 (2 µl/well) (Invitrogen) according to the manufacturer’s instructions. Following incubation for 4 hr at 37 °C, the cells were collected, lysed and the transfected DNA was captured and denatured as described before (“Selection of a transfection agent” section of this chapter).

Gel Analysis of DNA Recovered following Capture and Denaturation

The supernatant containing the DNA recovered following denaturation of the captured DNA was heated at 90 °C for 5 min in an 80% (vol/vol) formamide loading buffer (Teknova) and immediately loaded on a 12% TBE-polyacrylamide 8.3 M urea gel. The gel was run at 12 W for around 30 min, after which it was stained with SYBR® Green II (Invitrogen) according to manufacturer’s instructions. The DNA bands were visualized using 300 nm UV illumination. A 10 bp DNA ladder (Integrated Technologies) was also included.

Preparation and Gel Analysis of Untransfected SUM149PT Cell Controls

SUM149PT cells were plated in two wells of a 24-well plate as described before (“Selection of a transfection agent” section of this chapter). Both wells of cells were

treated with Lipofectamine™ 2000 (2 µl/well) according to manufacturer's instructions, and incubated for 4 hr at 37 °C in a CO₂ incubator. Cells from both the wells were lysed, and the lysate from only one well of cells was subjected to bead capture and denaturation as described before ("Selection of a transfection agent" section of this chapter). The supernatant obtained following denaturation, along with the lysate from the other batch of SUM149PT cells were electrophoresed on a 12% polyacrylamide 8.3 M urea gel at 110 V. The electrophoresed DNA bands were stained using SYBR® Green II, and visualized using 300 nm UV illumination. A 10 bp DNA ladder (Integrated Technologies) was also included.

Results

Substrate and Control DNA Oligonucleotides

The 8oxodG BER assay uses a double-stranded oligonucleotide DNA substrate (also represented as “+ 8oxodG/biotinylated DNA”) that consists of a biotinylated DNA strand (nontarget strand) that is base paired to an untagged DNA strand containing a single 8oxodG lesion (+8oxodG or target strand). A double-stranded control DNA (also represented as “- 8oxodG/biotinylated DNA”) that is identical to the substrate DNA, except that it has a guanine instead of the 8oxodG lesion on the untagged strand (-8oxodG or control strand), was used for the optimization experiments.

Overview of the in vivo 8oxodG BER Assay

In the first step, the substrate DNA is transfected into target cells and incubated for an increasing period of time to allow repair of the 8oxodG lesion. The cells are then lysed and the biotinylated substrate DNA is captured using streptavidin-coated magnetic beads. In the presence of a magnet, the strand containing the 8oxodG lesion (+8oxodG or target strand) is denatured and isolated from the streptavidin-bound biotinylated strand (nontarget strand). The isolated DNA is then quantified and subjected to an 8oxodG competitive ELISA to measure the disappearance of 8oxodG lesions over time (Figure 7).

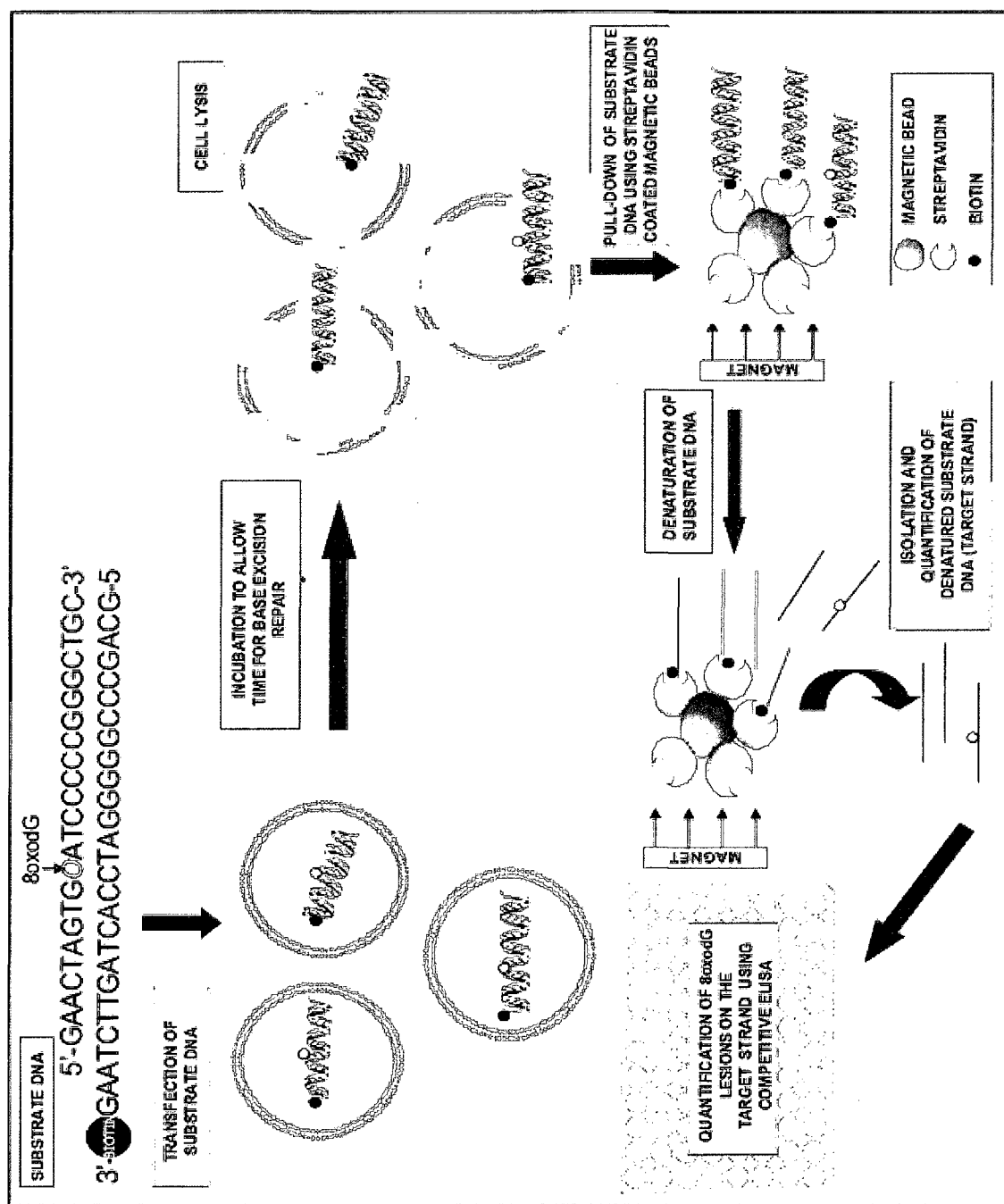


Figure 7. Overview of the in vivo 8oxodG BER assay

Gel Analysis of the Single-Stranded DNA Oligonucleotides

In order to verify the lengths of the synthesized single-stranded DNA oligonucleotides, and to establish the experimental conditions for the denaturing gel electrophoresis, the +8oxodG, -8oxodG and biotinylated DNA oligonucleotides were electrophoresed on a denaturing gel (Figure 8) prior to being used for preparation of the substrate and control DNA.

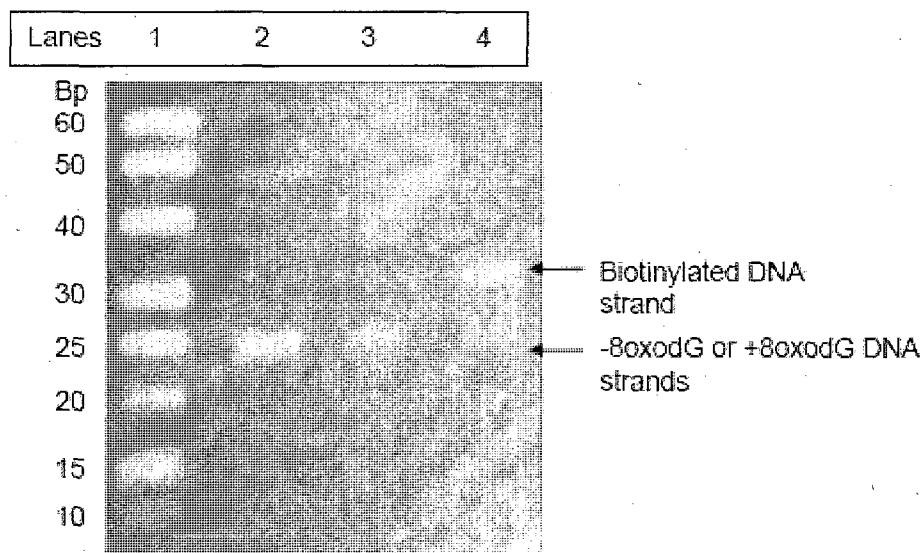


Figure 8. Gel analysis of the single-stranded DNA oligonucleotides used in the in vivo 8oxodG BER assay. The single-stranded -8oxodG, +8oxodG and biotinylated DNA oligonucleotides (50 ng) were denatured by heating at 90 °C for 5 min in 95% (vol/vol) formamide. The samples were loaded on a 15% TBE-polyacrylamide 7 M urea gel, stained using SYBR® Green II and visualized using 300 nm UV illumination. Lane 1: 10 bp DNA ladder; lane 2: -8oxodG DNA strand; lane 3: +8oxodG DNA strand; lane 4: biotinylated DNA strand.

On electrophoresis, the 24-mer -8oxodG DNA (lane 2) and +8oxodG DNA (lane 3) oligonucleotides were found to comigrate with and slightly above a 25-mer DNA

marker, respectively. We believe that the +8oxodG strand migrated slower than expected due to the presence of the 8oxodG lesion. Besides the 24-mer band, a faint band which was around 50 bases in length was also observed in the -8oxodG DNA lane. This was probably formed due to the self-annealing of the 24-mer -8oxodG DNA strands, since the DNA has self-complementary regions of guanine and cytosine bases. The 28-mer biotinylated DNA strand (lane 3) was found to migrate slightly above a 30-mer DNA marker. The slower migration was probably due to the presence of the biotin tag. Both the +8oxodG and biotinylated DNA were found to stain less strongly with the SYBR[®] Green II dye when compared to the -8oxodG DNA. Due to their high tendency to donate electrons, guanine bases have been shown to be efficient fluorescence quenchers (Lacowicz, 2006). The 8oxodG bases have an oxidation potential that is approximately 0.5 V lower than that of guanine (Stover, Ciobanu, Cliffler, & Rizzo, 2007). Thus, we believe that the low oxidation potential of the 8oxodG lesion in the +8oxodG DNA may quench the fluorescence of the dye. We also speculate that the presence of the biotin tag in the biotinylated DNA reduces the surface adsorption of the monomeric dye to the DNA.

Preparation of Substrate and Control DNA

The substrate and control DNA were prepared by annealing the single-stranded +8oxodG and -8oxodG oligonucleotides respectively to the biotinylated DNA oligonucleotide in a 2:1 ratio. This ratio was used to ensure the annealing of all the biotinylated DNA strands, so that they would not compete with the annealed substrate or

control DNA for binding to the streptavidin-coated beads during the optimization experiments. The annealed substrate and control DNA were quantified using SYBR[®] Green I, since this dye binds preferentially to the minor groove of double-stranded DNA (Zipper, Brunner, Bernhagen, & Vitzthum, 2004). Following annealing, the DNA was analyzed on a 15% nondenaturing polyacrylamide gel (Figure 9).

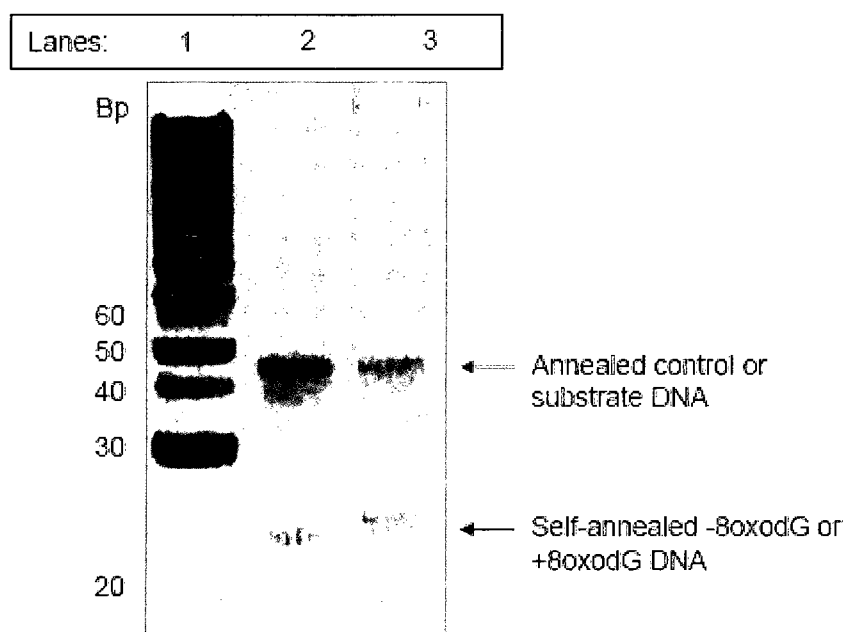


Figure 9. Gel analysis of the annealed double-stranded substrate and control DNA. The annealed substrate and control DNA (25 ng each) were electrophoresed on a 15% TBE-polyacrylamide gel. The gel was stained using SYBR[®] Green I and visualized using 300 nm UV illumination. Lane 1: 10 bp DNA ladder; lane 2: annealed control ds DNA; lane 3: annealed substrate ds DNA. ds = double-stranded

Following annealing, we would expect three species of DNA on the nondenaturing gel: (a) the annealed double-stranded substrate or control DNA, (b) self-annealed (~24 bp) +8oxodG or -8oxodG DNA (since this was used in excess of

the biotinylated DNA for the annealing), and (c) self-annealed (~28 bp) biotinylated DNA (if annealing was not 100%). Two bands were seen in both the annealed substrate and control DNA lanes; one band was approximately 24 bp in length and the other was approximately 45 bp in length. We believe that the 24 bp band corresponds to the self-annealed +8oxodG or -8oxodG DNA, and the 45 bp band corresponds to the annealed substrate or control DNA. No band approximately 28 bases in length (corresponding to self-annealed biotinylated DNA) was observed in the gel. This suggests that either all the biotinylated DNA was annealed (which would then suggest that the annealing was 100% successful), or the amount of biotinylated DNA in the gel was below the limit of sensitivity of the SYBR[®] Green I dye. In the future, it may be useful to determine the extent of annealing by monitoring the hyperchromicity shift at 260 nm.

Specificity of the 8oxodG Competitive ELISA

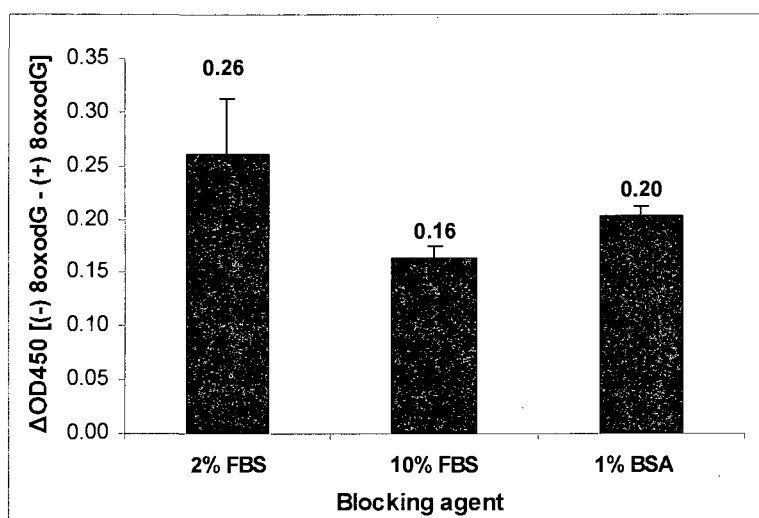
Since the HT 8oxodG ELISA Kit (Trevigen) was originally developed for the quantification of 8oxodG lesions in urine and serum samples, the specificity and efficiency of the ELISA when used with the oligonucleotides in our BER assay was first evaluated. Specificity of the 8oxodG ELISA may be defined as its ability to discriminate between DNA containing 8oxodG lesions and DNA lacking the lesions. Thus, in order to monitor ELISA specificity, the single-stranded +8oxodG DNA containing the 8oxodG lesion and the -8oxodG DNA lacking the lesion were used as positive and negative controls respectively.

In order to determine the amount of +8oxodG and -8oxodG DNA to be used for monitoring specificity, we first had to determine the range of DNA concentrations that could be used with the 8oxodG ELISA, so that the 8oxodG levels quantified are within the detection range of the ELISA. The preestablished sensitivity of the 8oxodG ELISA was 1.9 ng of 8oxodG/ml, and its detection range was 1.875-60 ng of 8oxodG/ml (Trevigen). Thus, the 8oxodG detection range in the 50 μ l assay volume (per well) was between 0.09375-3 ng of 8oxodG lesions. We calculated that 1 ng of our +8oxodG DNA had 0.04683 ng of 8oxodG lesions. Thus, the range of +8oxodG DNA that may be used in the 8oxodG ELISA was between 2-64 ng/well. To determine the specificity of the ELISA and to optimize its conditions, from this range, we used 5 ng/well of +8oxodG and -8oxodG DNA oligonucleotides. This was chosen to minimize the amount of DNA to be used in the BER assay. The specificity of the ELISA was measured as the difference in absorbance values (Δ OD450) obtained for equal amounts of +8oxodG and -8oxodG DNA. The higher the specificity of the assay the greater the difference in absorbance values between the two DNA.

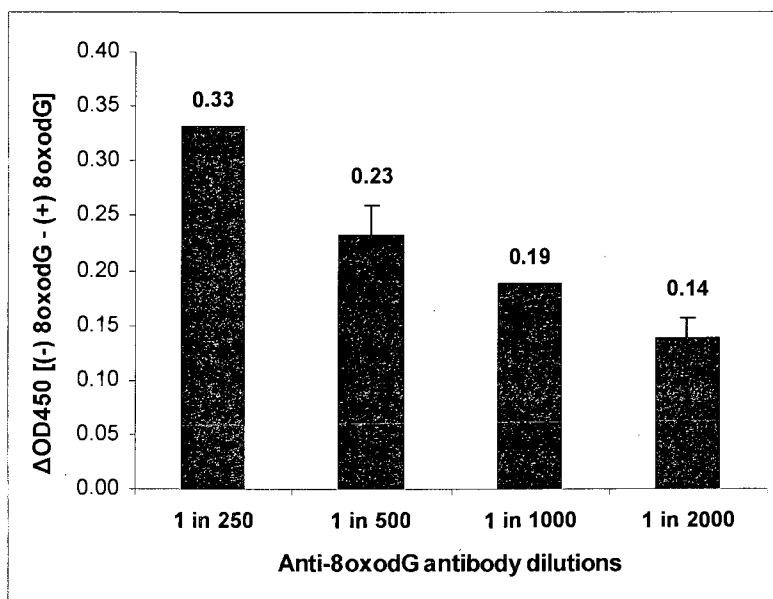
First, the specificity of the ELISA was monitored in the presence of two blocking agents: FBS (2% and 10% [vol/vol]) and BSA (1% [wt/vol]) (Figure 10A). Incubation of the wells with 2% FBS (150 μ l/well) for 1 hr at 37 $^{\circ}$ C gave the highest specificity (Δ OD450 = 0.26). Second, in order to identify the optimal concentration of anti-8oxodG antibody, the specificity of the ELISA was monitored at increasing (1/250, 1/500, 1/1000, 1/2000) primary antibody dilutions (Figure 10B). A 1/250 dilution of the primary antibody gave the highest specificity (Δ OD450 = 0.33). Third, to determine the optimal

incubation temperature following the addition of the anti-8oxodG antibody to the +8oxodG or -8oxodG DNA in the wells, the specificity of the ELISA was monitored at different incubation temperatures (25 °C and 37 °C) (Figure 10C). Room temperature incubation gave higher specificity when compared to that at 37 °C ($\Delta OD_{450} = 0.33$).

A.



B.



C.

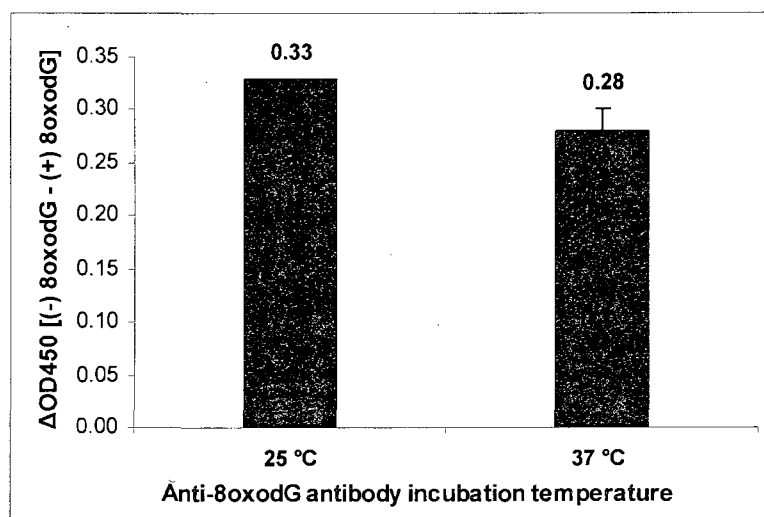


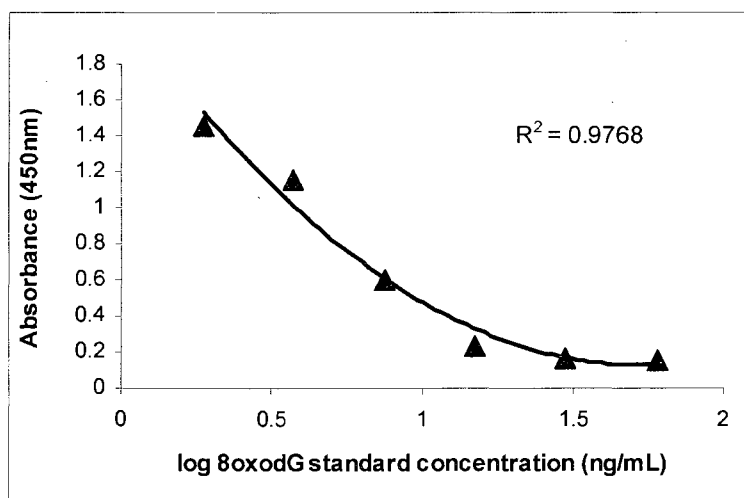
Figure 10. Specificity of the 8oxodG ELISA at different assay conditions. The +8oxodG and -8oxodG DNA (5 ng each) were subjected to the 8oxodG ELISA after blocking the wells (A) with either 2% FBS, 10% FBS or 1% BSA for 1 hr at 37 °C, or at different dilutions of the anti-8oxodG antibody (B), or using different temperatures for incubation of the anti-8oxodG antibody with the single-stranded +8oxodG or -8oxodG DNA (C). The specificity was measured as the difference in end absorbance values (ΔOD_{450}) obtained by subtracting the OD450 values of + 8oxodG DNA from those of the -8oxodG DNA. The higher the assay specificity, the greater will be the difference in absorbance values between the two DNA. The vertical lines depict the standard deviation. The bars lacking vertical lines represent the means for which the standard deviation was zero.

Efficiency of the 8oxodG Competitive ELISA

The efficiency of the 8oxodG ELISA was determined using the optimal assay conditions established in previous experiments (Figure 10 A, B, C). The amount of 8oxodG lesions quantified in 5 ng of +8oxodG DNA from two independent experiments (done using two different ELISA plates) were 0.1187 ng and 0.0982 ng of 8oxodG lesions. The average amount of 8oxodG lesions determined for the two experiments was 0.1085 ng lesions. The standard curve and sample absorbance values from one representative experiment have been shown in Figure 11. The figure also shows that the

average absorbance for the -8oxodG DNA strand was near that observed for the 0 ng/ml standard.

A.



B.

| Concentration of 8oxodG standards | Average absorbance (OD 450 nm) |
|--------------------------------------|-----------------------------------|
| 60 ng/ml | 0.160 |
| 30 ng/ml | 0.172 |
| 15 ng/ml | 0.238 |
| 7.5 ng/ml | 0.603 |
| 3.75 ng/ml | 1.156 |
| 1.875 ng/ml | 1.458 |
| 0 ng/ml | 1.672 |

C.

| Samples | Average absorbance (OD 450 nm) |
|-------------|-----------------------------------|
| -8oxodG DNA | 1.650 |
| +8oxodG DNA | 1.342 |

Concentration of 8oxodG lesions in
5 ng of +8oxodG DNA = 2.375 ng/ml

Figure 11. Efficiency of the 8oxodG competitive ELISA. The standard curve (A), average absorbance (OD450) values of the standards (B), and average OD450 values of the -8oxodG DNA (5 ng) and +8oxodG DNA (5 ng) (C) are shown. The concentration of 8oxodG lesions in the +8oxodG DNA was determined using the standard curve. The results shown are representative of two independent experiments.

We had previously calculated that 0.04683 ng of 8oxodG lesions are present in 1 ng of +8oxodG DNA. Thus, we theoretically expected 0.2342 ng of 8oxodG lesions in 5 ng of the +8oxodG DNA. Since the ELISA detected only 0.1085 ng of the lesions in 5 ng of the +8oxodG DNA, its efficiency was approximately 46.33%.

Once the efficiency was determined, the range of +8oxodG DNA concentrations that could be used with the 8oxodG ELISA was recalculated; the theoretical amount of +8oxodG DNA that may be used after correction for ELISA efficiency is 4.3-138.4 ng/well.

In vitro Validation of the 8oxodG Competitive ELISA for Use in the BER Assay

At the end of the capture and denaturation step in the BER assay, the supernatant isolated is likely to have the following DNA species: repaired +8oxodG DNA strands (no 8oxodG lesions), and unrepaired +8oxodG DNA strands (with 8oxodG lesions).

Depending on the efficiency of BER in the target cells, the ratio of repaired to unrepaired +8oxodG DNA may range from 1:0 to 0:1. We wanted to see if the 8oxodG ELISA was capable of effectively measuring 8oxodG lesions in the unrepaired DNA, against a background of repaired DNA. Thus, we attempted to simulate the outcome of the BER assay in order to validate the 8oxodG ELISA for use with the assay.

In this experiment, the -8oxodG DNA strand was used to represent repaired DNA and the +8oxodG DNA strand was used to represent the unrepaired DNA. The -8oxodG DNA strands were spiked with an increasing amount of +8oxodG DNA, while keeping the total amount of DNA constant (100 ng) (Table 2). The amounts of +8oxodG DNA used were within the theoretical detection range of the ELISA (4.3-138.4 ng/well). The ability of the ELISA to detect increasing amounts of 8oxodG lesions in the +8oxodG DNA (unrepaired DNA) against a background of -8oxodG DNA (repaired DNA) was then determined (Figure 12).

The 8oxodG ELISA showed the ability to detect and quantify 8oxodG lesions on the +8oxodG DNA in a dose-dependent manner, in the presence of different amounts of -8oxodG DNA. This suggests that the presence of the repaired DNA will not interfere with the quantification of lesions on the unrepaired DNA (at least when the total amount of repaired and unrepaired DNA together is ≤ 100 ng). Thus, the 8oxodG ELISA may be

used in the BER assay to measure the decrease in the amount of 8oxodG lesions on the +8oxodG DNA, seen with time. This experiment may be used in the future to generate a standard curve to estimate the amount of repaired versus unrepaired target DNA recovered from the target cells.

Table 2

Amount of +8oxodG and -8oxodG DNA used for the in vitro validation of the 8oxodG ELISA

| Amount of +8oxodG DNA per well (ng) | Amount of -8oxodG DNA per well (ng) | Total amount of DNA per well (ng) |
|--|--|--------------------------------------|
| 0 | 100 | 100 |
| 6.25 | 93.75 | 100 |
| 12.5 | 87.5 | 100 |
| 25 | 75 | 100 |
| 50 | 50 | 100 |
| 100 | 100 | 100 |

Note. An increasing amount of +8oxoG DNA was loaded in triplicate wells of the 8oxodG ELISA plate. The -8oxodG DNA was added to these wells such that the total amount of DNA in each well was 100 ng. The DNA was then subjected to the 8oxodG ELISA and the concentration of 8oxodG lesions in each well was determined.

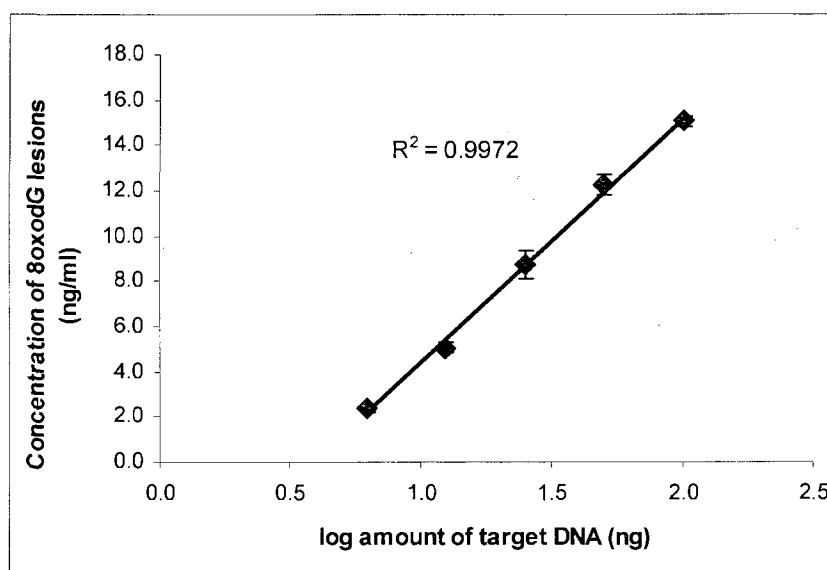


Figure 12. Dose-dependent detection of 8oxodG lesions on the +8oxodG DNA in the presence of the -8oxodG DNA. The -8oxodG was spiked with an increasing amount of +8oxodG (target) DNA so that the final amount of DNA in each well was 100 ng. The 8oxodG lesions were detected and quantified using the HT 8oxodG ELISA Kit as described in the Methods section. The data points represent the mean concentration of 8oxodG lesions. The vertical lines represent the standard deviation.

Titration of the Amount of Streptavidin-Coated Magnetic Beads to Use in the BER Assay

In the BER assay, following lysis of the cells transfected with the biotin-tagged substrate or control DNA, the transfected DNA will have to be captured using streptavidin-coated magnetic beads. In order to determine the optimal amount of beads required to effectively capture the transfected substrate or control DNA following cell lysis, a titration using different bead concentrations was performed.

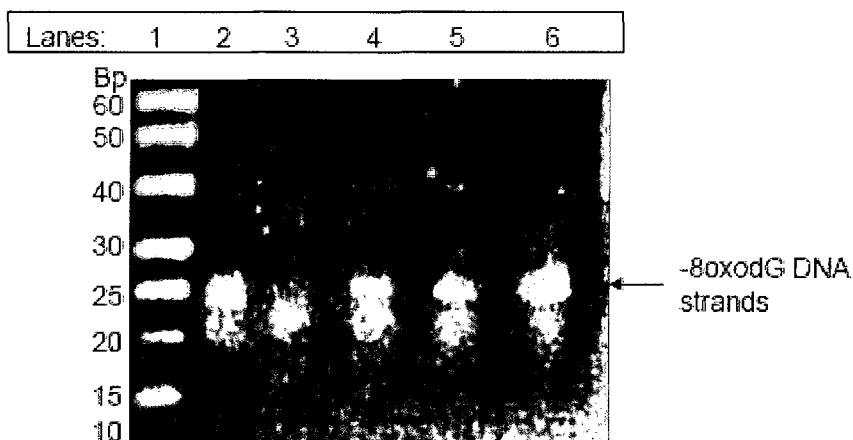
Double-stranded control (-8oxodG/biotinylated) DNA (100 ng), and different amounts of beads (10 μ g, 50 μ g, 100 μ g, 150 μ g) were used for the titration. Following binding of the control DNA to the beads, the DNA was denatured using 0.1 M sodium hydroxide, and the supernatant was collected in the presence of a magnet. This step

would, in theory, isolate the -8oxodG DNA strand from the biotinylated DNA strand bound to the beads. The DNA isolated from each of the four experiments that used different amounts of beads were then analyzed on a denaturing gel (Figure 13A) after staining with SYBR[®] Green II.

The intensity of the 24-mer DNA bands obtained for the DNA isolated from each of the four experiments, and the reference DNA band (11 ng of -8oxodG DNA strand) were determined using the Image J software (Figure 13B). The band intensities of the samples were then expressed as a percentage of the band intensity of the reference DNA. Since the amount of DNA in the reference band was known (11 ng), the amount of DNA in each band from the sample lanes (lanes 3-6) was estimated. Using these data, the total amount of DNA isolated from each of the four bead capture experiments was estimated (Figure 13B).

The expected amount of isolated single-stranded -8oxodG DNA from 100 ng of double-stranded control DNA, following denaturation, was 50 ng. Approximately 13.98 ng, 20.41 ng, 41.66 ng and 52.05 ng of single-stranded control DNA was isolated from 10 μ g, 50 μ g, 100 μ g, and 150 μ g of bead-DNA suspension respectively, following denaturation. From the titration performed, 150 μ g of streptavidin-coated magnetic beads was determined to be the optimal amount of beads that could bind 100 ng of substrate or control DNA. Thus, the optimal ratio of the amount of substrate or control DNA to the amount of streptavidin-coated beads to be used was estimated to be approximately 1 ng DNA to 1.5 μ g beads.

A.



B.

| | | DNA isolated following titration of streptavidin-coated magnetic beads | | | |
|---|------|---|------------|-------------|-------------|
| Reference Band | | 10 μ g | 50 μ g | 100 μ g | 150 μ g |
| Band Intensity | 2078 | 528 | 771 | 1574 | 1966 |
| Relative band intensity | 1 | 0.254 | 0.371 | 0.757 | 0.946 |
| Amount of DNA per band (ng/5 μ l) | 11 | 2.795 | 4.081 | 8.332 | 10.407 |
| Amount of DNA in the supernatant (ng/25 μ l) | | 13.98 | 20.41 | 41.66 | 52.05 |

Figure 13. Titration of the amount of streptavidin-coated magnetic beads required to capture the control DNA. The control DNA (100 ng) was mixed with streptavidin-coated magnetic beads (10 μ g, 50 μ g, 100 μ g, 150 μ g) and incubated as described in the Methods section. The DNA captured by the beads was then denatured using 0.1 M sodium hydroxide in the presence of a magnet, and the DNA in the supernatant was isolated. The isolated DNA was analyzed on a 12% TBE-polyacrylamide 8.3 M urea gel (A) following denaturation by heating at 90 °C in 95% (vol/vol) formamide. Lane 1: 10 bp DNA ladder; lane 2: Reference band (-8oxodG DNA strand); lane 3, 4, 5, 6: DNA

isolated following capture and denaturation of control DNA using 10 μ g, 50 μ g, 100 μ g, and 150 μ g beads respectively. The band intensities were determined using Image J software (B) and the amount of DNA in each band and in the eluted supernatant was calculated from the known amount of DNA in the reference band.

The gel (Figure 13A) also showed that only the -8oxodG DNA strand (24-mer) and not the biotinylated DNA strand (28-mer) was isolated following bead capture and denaturation. Thus, treatment with 0.1 M sodium hydroxide did not disrupt the streptavidin-biotin linkages. As seen in Figure 8, an additional band (~40-mer) was seen in all the lanes. As mentioned before, it is believed that this band is due to self-annealing of the -8oxodG DNA strands.

Selection of a Suitable Fluorescent Dye for the Quantification of the Isolated DNA in the BER assay

In the BER assay, following capture and denaturation of the transfected substrate DNA, the isolated DNA containing the +8oxodG DNA strand will have to be quantified prior to being used in the 8oxodG ELISA. Two fluorescent dyes (SYBR[®] Green II and Quant-iT[™] Oligreen) were evaluated for their efficiency in quantifying single-stranded DNA. The single-stranded -8oxodG DNA was used to generate standards ranging from 0-50 ng/ml (in 10 ng/ml increments). The R^2 values of the standard curve generated using the same set of standards and measured using each of the two dyes were then compared. The Quant-iT[™] Oligreen dye gave better R^2 value for the standard curve ($R^2 = 0.9982$) when compared to the SYBR[®] Green II dye ($R^2 = 0.8877$). Similar results were obtained when using standards ranging from 0-25 ng/ml (in 5 ng/ml increments); the R^2 value for the standard curve using Quant-iT[™] Oligreen dye and SYBR[®] Green II

dye was 0.9969 and 0.7291 respectively. Thus, the Quant-iT™ Oligreen fluorescent dye was chosen for the quantification of the isolated DNA following denaturation in the BER assay.

Transfection of the Substrate or Control DNA into Target Cells

The first step of the BER assay involves the transfection of the substrate DNA into target cells. Since the assay was being developed to confirm the results observed from the first part of our study (described in chapter one), we used SUM149PT cells to determine conditions for substrate or control DNA transfection. Double-stranded control DNA (-8oxodG/biotinylated DNA) was used in the optimization experiments.

Two different transfection reagents (Lipofectamine™ 2000 and Oligofectamine™) were first compared for their efficiency in transfection of the control DNA into the target cells. No cytotoxicity was observed among the untransfected cells that were treated only with either of the two reagents (2 µl of reagent per well of a 24-well plate). Since transfection of biotin-tagged oligonucleotides has not been reported previously, we decided to use a large amount of control DNA for the transfection to first verify if the biotin-tagged DNA can successfully transfect cells. Thus 800 ng of control DNA was transfected using either of the two reagents (2 µl of reagent per well) into SUM149PT cells. Following 4 hr of incubation, the cells were lysed. To prevent the denaturation of the biotin moiety in the control DNA, a nonionic detergent-based cell lysis buffer was used. Since the optimal ratio of the amount of substrate or control DNA to the amount of streptavidin-coated beads was previously

determined to be 1 ng DNA to 1.5 μ g beads (Figure 13), 850 μ g of beads were used to capture the control DNA (800 ng) from the cell lysate. The captured DNA was then denatured in the presence of a magnet, and the DNA recovered in the supernatant was quantified using the Quant-iT™ Oligreen dye. The concentration of DNA in the eluted supernatant was approximately the same for cells transfected with Lipofectamine™ 2000 (0.27 ng/ μ l) and Oligofectamine™ reagent (0.25 ng/ μ l) (Figure 14). Since Lipofectamine™ 2000 is a more commonly used reagent, we decided to use this for future experiments.

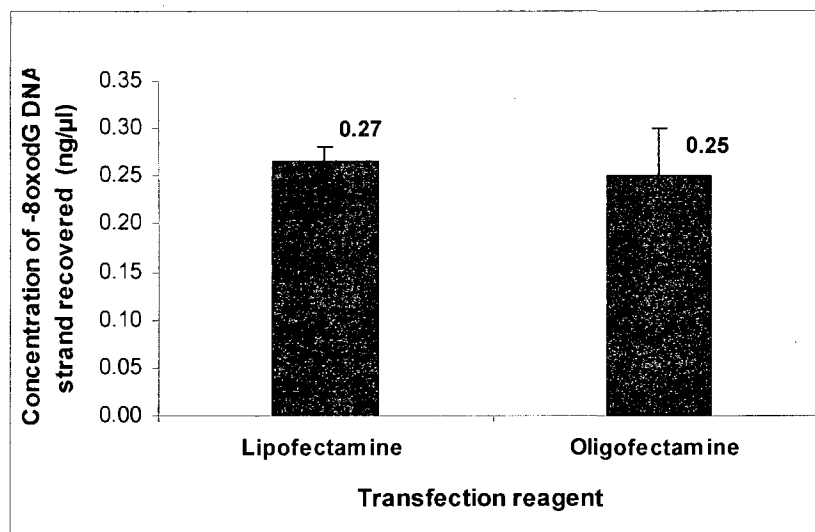


Figure 14. Selection of a suitable transfection reagent for the BER assay. SUM149PT cells were transfected with the control DNA (800 ng) using 2 μ l/well of either the Lipofectamine™ 2000 or Oligofectamine™ transfection reagent. The cell lysis, capture and denaturation steps were performed as described in the Methods section. The DNA recovered in the supernatant following denaturation, was quantified using the Quant-iT™ Oligreen dye. The bars represent the mean concentrations of DNA recovered from two independent experiments. The vertical lines represent standard errors of the means.

Following selection of a suitable transfection reagent, the optimal volume of the reagent to use for transfection was then determined. Out of three different volumes of Lipofectamine™ 2000 tested (2, 4, or 6 µl of reagent per well of a 24-well plate), the concentration of the recovered DNA was the highest when 2 µl of Lipofectamine™ 2000 was used for transfection of SUM149PT cells (Figure 15). No cytotoxicity was observed in the transfected cells (with 800 ng control DNA) or untransfected cell controls (treated only with 2, 4, or 6 µl of Lipofectamine™ 2000), following incubation for 4 hr at 37 °C. This shows that neither the reagent, nor the combination of reagent with DNA were cytotoxic to the cells at the concentrations used and the time incubated.

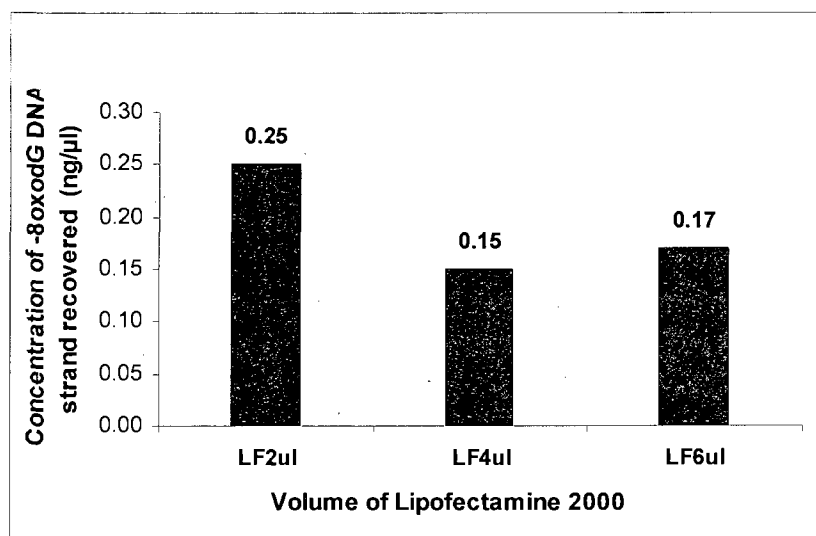


Figure 15. Optimal volume of Lipofectamine™ 2000 for use in the transfection step of the BER assay. The SUM149PT cells were transfected with control DNA (800 ng) using either 2 µl, 4 µl or 6 µl of Lipofectamine™ 2000. The cell lysis, capture and denaturation steps were performed as described in the Methods section. The DNA eluted in the supernatant following denaturation was quantified using the Quant-iT™ Oligreen dye. LF = Lipofectamine™ 2000.

Gel Analysis of the DNA Recovered following Transfection of Substrate or Control DNA into SUM149PT and MCF7 Cells

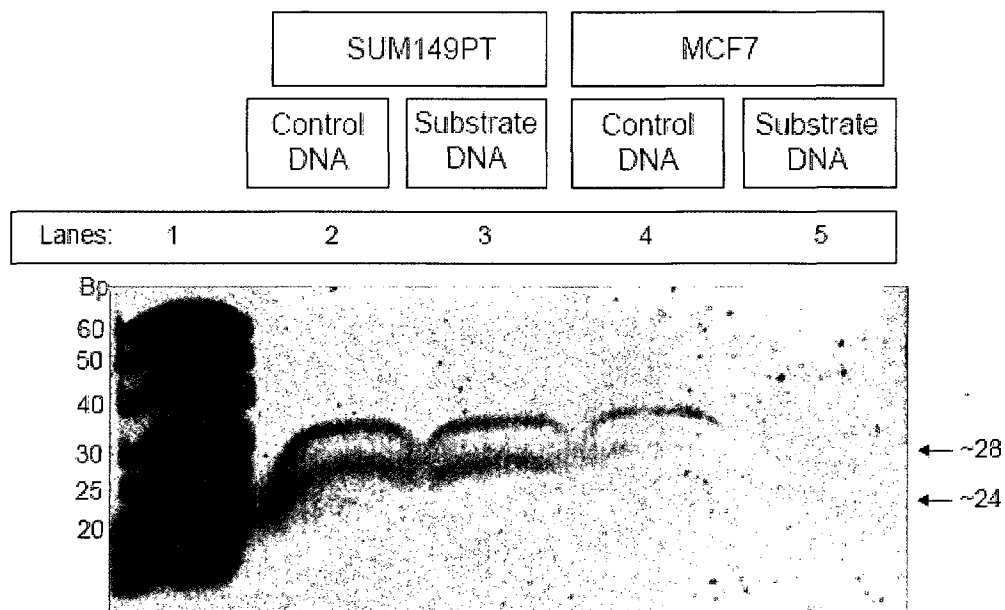
Following transfection of substrate DNA (+8oxodG/biotinylated DNA) into target cells, incubation, cell lysis, bead capture and denaturation in the presence of a magnet, the recovered DNA should only consist of the +8oxodG DNA strand (Figure 7). To confirm that the DNA recovered following transfection of the substrate DNA into SUM149PT cells consisted only of the +8oxodG DNA strands, the transfection was performed in SUM149PT cells using substrate DNA (800 ng) and Lipofectamine™ 2000. In addition, another batch of SUM149PT cells was transfected with the control DNA (800 ng) instead of the substrate DNA. Following incubation for 4 hr, and cell lysis, the transfected substrate and control DNA were captured, denatured, and the supernatant was collected in the presence of a magnet. Equal volumes of the supernatant from each transfection were electrophoresed on a denaturing gel (Figure 16A, lanes 2, 3). The gel showed one band that corresponds to the 28-mer biotinylated DNA and another band that corresponds to the 24-mer +8oxodG or -8oxodG DNA. Both the bands were observed in the DNA recovered following transfection of the control DNA (Fig 16A, lane 2) and the substrate DNA (Fig 16A, lane 3) into SUM149PT cells. In addition to these two bands, a third band, approximately 50 bases in length, was seen only in the DNA recovered following transfection of the control DNA (Fig 16A, lane 2). We speculated that this 50-mer was formed due to self-annealing of the -8oxodG DNA strands, as was previously observed on gel electrophoresis of single-stranded -8oxodG DNA (Figure 8). The absence of this 50-mer band in the DNA recovered following transfection of the substrate

DNA (Fig 16A, lane 3) is also consistent with the observations from electrophoresis of the single-stranded +8oxodG DNA in Figure 8.

The substrate and control DNA were also transfected into another cell line (MCF7), to show that the bands observed were not cell-type specific and to also demonstrate that the substrate or control DNA could be transfected into other cell lines. Following gel electrophoresis, the DNA recovered following transfection of the control DNA (Figure 16A, lane 4) and the substrate DNA (Figure 16A, lane 5) into MCF7 cells produced bands identical to those observed from the transfections in the SUM149PT cells (Figure 16A, lanes 2, 3).

To further confirm that the DNA bands observed in Figure 16A were specific for the transfected DNA, we prepared two sets of untransfected SUM149PT cells. Both sets of cells were lysed. The lysate from one set of cells, on electrophoresis, showed a smear of DNA (Figure 16B, lane 2). No bands corresponding to the substrate or control DNA (24, 28 bases) were seen. The lysate from the other set of untransfected SUM149PT cells was subjected to bead capture and denaturation. On electrophoresis of the denatured supernatant, no bands were observed (Figure 16B, lane 3). Nanodrop spectrophotometry of this denatured supernatant also confirmed the absence of DNA (data not shown). This suggested that no DNA was isolated on subjecting the untransfected SUM149PT cells to lysis, bead capture and denaturation. Taken together with the data obtained in Figure 16A, we concluded that the DNA recovered from the cell lysates of SUM149PT and MCF7 cells transfected with the substrate and control DNA consisted only of the transfected DNA.

A



B.

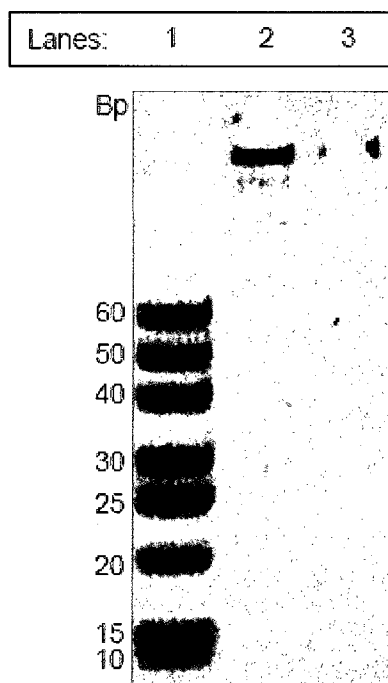


Figure 16. Transfection of control and substrate DNA into SUM149PT and MCF7 cells. SUM149PT and MCF7 cells were transfected with the control or substrate DNA (800 ng) using Lipofectamine™ 2000 (A). The cell lysis, capture and denaturation steps were

performed as described in the Methods section. The DNA eluted in the supernatant was run on a 12% polyacrylamide 8.3 M urea gel. Lane 1: 10 bp DNA ladder; lanes 2, 3: DNA recovered following transfection of SUM149PT cells with control DNA and substrate DNA respectively; lanes 4, 5: DNA recovered following transfection of MCF7 cells with control DNA and substrate DNA respectively. Cell lysates from untransfected SUM149PT cells (B) were either used as is (Panel B, lane 2), or subjected to bead capture and denaturation (Panel B, lane 3), prior to being electrophoresed. A 10 bp DNA ladder (Panel B, lane 1) is also shown.

Consequences of the Coelution of the Biotinylated DNA Strand with the +8oxodG or -8oxodG DNA strand following Denaturation of Captured Substrate or Control DNA

Figure 16A showed that the +8oxodG or -8oxodG DNA strand (24-mer) and the biotinylated DNA strand (28-mer) were present in the supernatant following bead capture of transfected DNA and denaturation. The presence of the biotinylated DNA strand in the supernatant was unexpected since we had previously observed that when using similar bead capture and denaturation conditions, the biotinylated strand did not coelute with the +8oxodG or -8oxodG DNA strand (Figure 13). Figure 16A also showed that the amount of biotinylated DNA that coeluted with the +8oxodG or -8oxodG DNA strands in each of the four transfection experiments (Figure 16A, lanes 2-5) was consistent (as visualized by the band intensity). This suggested that as long as the DNA capture, denaturation and recovery steps are consistently performed following every transfection experiment, the percentage of coeluted biotinylated DNA (if any) that is recovered from every experiment would be similar. Thus, if the presence of the biotinylated DNA did not compromise the efficiency of the 8oxodG ELISA to quantify lesions on the +8oxodG DNA, its coelution may be overlooked. To verify this, the ability of the ELISA to detect and quantify 8oxodG lesions on increasing amounts of +8oxodG DNA, in the

absence/presence of an equal amount of the biotinylated DNA was monitored (Table 3, Figure 17).

Table 3

Amount of biotinylated DNA and/or +8oxodG DNA used to determine the efficiency of the 8oxodG ELISA

| A. | B. | |
|-------------------|-------------------|------------------------|
| Amount of +8oxodG | Amount of +8oxodG | Amount of biotinylated |
| DNA per well (ng) | DNA per well (ng) | DNA per well (ng) |
| 0 | 0 | 0 |
| 6.25 | 6.25 | 6.25 |
| 12.5 | 12.5 | 12.5 |
| 25 | 25 | 25 |
| 50 | 50 | 50 |
| 100 | 100 | 100 |

Note. An increasing amount of +8oxodG DNA was loaded in triplicate wells of the 8oxodG ELISA plate (A). An increasing amount of +8oxodG DNA spiked with an equal amount of biotinylated DNA was also loaded in triplicate wells of the 8oxodG ELISA plate (B). The DNA was then subjected to the 8oxodG ELISA and the concentration of 8oxodG lesions in each well was determined.

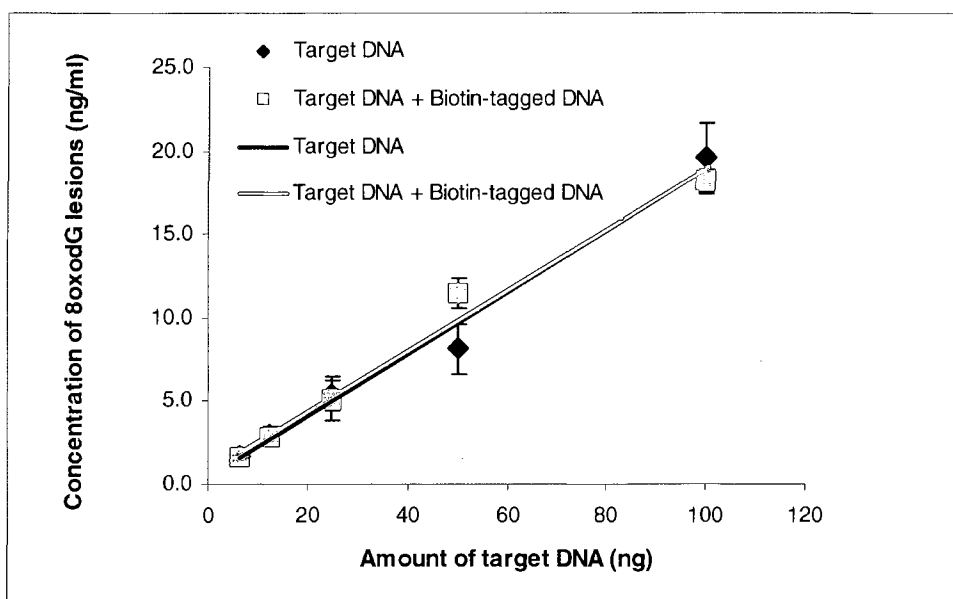


Figure 17. Quantification of 8oxodG lesions on the +8oxodG DNA in the presence or absence of the biotinylated DNA. Increasing amounts of +8oxodG (target) DNA strand were subjected to the 8oxodG ELISA with or without equal amounts of biotinylated DNA strand. The concentration of 8oxodG lesions on the +8oxodG DNA strand in the absence (black diamonds, black trendline) or presence (red squares, red trendline) of the biotinylated DNA strand was then determined.

The slopes of the trend lines (Figure 17) obtained for the concentration of 8oxodG lesions on-increasing amounts of +8oxodG DNA were similar in both the absence (slope = 0.186) and presence (slope = 0.181) of biotinylated DNA. Thus, the presence of the biotinylated DNA does not interfere with the quantification of 8oxodG lesions on the +8oxodG DNA strand and hence its coelution following capture and denaturation of the substrate DNA may be overlooked.

Discussion

Defects in the BER of 8oxodG lesions have been implicated in cancer (Paz-Elizur et al., 2003). The efficiency of BER of 8oxodG lesions in mammalian cells may be determined by monitoring the disappearance of 8oxodG levels in cellular DNA, following treatment with oxidizing agents. Techniques such as comet assays, immunoassays and HPLC-ECD that have been developed for this purpose suffer from issues related to their sensitivity, specificity and artifact production. Besides the HCR assay, currently, no other reliable assay to measure in vivo BER of 8oxodG lesions using DNA repair substrates is available. Thus, in this study, we have designed a novel in vivo assay for measuring BER of 8oxodG lesions using an oligonucleotide DNA substrate. This assay provides an advantage over the HCR assay because it detects the kinetics of BER, whereas the HCR assay is an end-point assay.

The double-stranded oligonucleotide DNA substrate used in our BER assay consists of an 8oxodG lesion on one strand and a 3' biotin tag on the complementary strand. The substrate DNA is transfected into target cells using Lipofectamine™ 2000 and incubated for an increasing period of time to allow for repair. The cells are then lysed using a nonionic cell lysis buffer and the lysate is treated with streptavidin-coated magnetic beads (DNA [ng]: bead [μg] ratio = 1:1.5), to allow the biotin-tagged substrate DNA to be captured from the cell lysate. Following DNA capture and washing to remove nonspecific DNA binding to the beads, the bead bound DNA is treated with 0.1 M sodium hydroxide to denature the untagged target strand from the biotin-tagged

nontarget strand (still bound to the beads). In the presence of a magnet, the bead bound nontarget strand is separated from the denatured target strands (in the supernatant). The DNA in the supernatant is then quantified by fluorimetry using the Quant-iT™ Oligreen fluorescent dye. Equal amounts of DNA from each time-point (the various time-points at which the target cells were incubated) are then subjected to an 8oxodG competitive ELISA, to quantify the amount of 8oxodG lesions on the target DNA. In vivo BER is measured as the disappearance of 8oxodG lesions with time.

The substrate DNA is a critical component of any repair assay. Thus, we first generated a list of specifications for selection of a suitable substrate DNA for our assay. Being an in vivo assay, the substrate DNA has to be transfected into cells. Thus, the substrate DNA should be double-stranded, with one or more 8oxodG lesions at predetermined position(s). It should also be easy to transfect into cells and be stable in vivo. Since the recognition of the lesions by hOGG1 followed by hOGG1- or APE1-mediated cleavage is a critical step in BER, the biochemistry of the substrate DNA chosen should not interfere with these steps. Following cell lysis, the DNA should be easily captured and purified, and form well characterized bands after gel electrophoresis.

As a first step, to make the choice between plasmid and linear oligonucleotide substrates, the advantages and disadvantages of each substrate in relevance to this assay were analyzed. Plasmid substrates can be transfected using common lipid-based reagents and are stable in vivo. In addition, plasmid substrates allow analysis of the long-patch BER (LP-BER) of base lesions, because the clamp protein proliferating cell-nuclear antigen (PCNA) required for LP-BER, functions only on circular DNA substrates (Biade,

Sobol, Wilson, & Matsumoto, 1998). On the other hand, the preparation and purification of plasmid DNA substrates containing 8oxodG lesions at predetermined positions (described by Hou, Prasad, Asagoshi, Masaoka & Wilson, 2007) is tedious. In addition, genomic DNA contamination may be introduced during the isolation of the plasmids from the cell lysate, following transfection and incubation in target cells.

Linear oligonucleotide DNA substrates on the other hand can be annealed from single-stranded commercially synthesized and purified strands. If tagged, the oligonucleotide DNA substrate can be easily captured and purified following cell lysis, without disrupting the 8oxodG lesions. However, the disadvantages of these substrates are that they do not allow repair using the LP-BER pathway, and their stability may be compromised *in vivo*. Studies conducted *in vitro* have shown that hOGG1-mediated repair of 8oxodG occurs almost exclusively along the short-patch BER (SP-BER) pathway (Dianov et. al., 1998; Fortini et. al., 2003). Thus, the use of a linear oligonucleotide DNA substrate to measure BER of 8oxodG lesions should not pose a problem. In addition, partially phosphorothionated substrate DNA may be used to maintain *in vivo* substrate stability. Thus, we decided to use a linear oligonucleotide DNA substrate for our BER assay.

The successful hOGG1-mediated incision of a commercially available (Trevigen) oligonucleotide, 24 bases in length, carrying a single 8oxodG lesion, has been shown before (Achanti & Huang, 2004). The study also used a 3' biotin tagged oligonucleotide that was complementary to the 8oxodG containing strand. Thus, the two oligonucleotides described by Achanti and Huang (2004), were chosen for our assay. To prevent

interference with enzyme binding and excision of the 8oxodG lesion on the target strand, the biotin moiety was tagged only to the complementary strand.

Denaturing gel electrophoresis of the purchased single stranded DNA oligonucleotides revealed bands of the expected sizes for the single-stranded +8oxodG DNA and biotinylated DNA (Figure 8). However, for the single-stranded -8oxodG DNA, besides a 24 base fragment, another fragment which was approximately 50 bases in length was observed. Although the +8oxodG DNA had the same sequence as the -8oxodG DNA plus an 8oxodG lesion, the 50-mer DNA band was not observed in the +8oxodG DNA lane. We speculated that this additional band was formed due to self-annealing of the -8oxodG DNA strands, and that this was not seen with the +8oxodG DNA strands because the 8oxodG lesion destabilized and thus prevented self-annealing. To test this hypothesis, we treated the -8oxodG DNA with higher formamide concentrations (98-100% [vol/vol]) to completely disrupt self-annealing, and electrophoresed the DNA in a denaturing gel. Following staining, the additional 50 base length band was not observed (data not shown). However, when this experiment was repeated, the band reappeared (data not shown). In the future, the identity of the fragment may be confirmed by excision of the band, elution of the DNA and sequencing.

Transfection of deoxyribonucleotides into cell cultures has been previously performed (Li, Dowbenko, & Lasky, 2002). However, no study to date has transfected biotin-tagged oligonucleotides into cell cultures. Thus, we first had to verify if the biotin-tagged substrate DNA could successfully be transfected into target cells. The double-stranded control DNA was used to optimize conditions for transfection because it

was identical to the substrate DNA, except for the absence of an 8oxodG lesion. The control DNA was transfected into SUM149PT cells using two different lipid-based transfectants. At the end of cell lysis, capture of the transfected DNA, and denaturation, the supernatant was collected and subjected to DNA quantification by fluorimetry. The analysis showed the presence of DNA in the supernatant (Figure 14). However, the species of DNA in the supernatant could not be verified by gel electrophoresis because the amount of DNA recovered was low. The transfection was then repeated in SUM149PT cells (with both control and substrate DNA), and this time the entire volume of supernatant isolated following bead capture of the lysate and denaturation was electrophoresed on a denaturing gel, to visualize the DNA recovered. The gel showed the presence of the DNA bands that corresponded to those of the substrate and control DNA (Figure 16A). The same results were obtained when the experiment was repeated using another cell line (MCF7). The use of two untransfected SUM149PT cell controls confirmed that the DNA bands observed were not endogenous to the cell lysate (Figure 16B). Taken together, these results confirmed that the biotin-tagged substrate and control DNA could indeed be transfected into cell cultures.

Although we did observe transfection of the substrate and control DNA, the percentage of transfected DNA recovered following cell lysis, capture and denaturation was low (~2.03%). This may be due to a number of reasons; failure of the oligonucleotide DNA substrate to enter the cells, their susceptibility to cytoplasmic, lysosomal, or other organellar DNases, the exocytosis of the DNA, or the loss of DNA during cell division (Lechardeur et al., 1999). To circumvent digestion by cellular

endo- and exonucleases, some of the phosphate groups in the oligonucleotide substrate may be modified by phosphorothioation in future experiments. It is however important not to modify phosphates that flank the 8oxodG lesion, so that the hOGG1- or APE1-mediated strand cleavage and other BER steps may proceed unhindered. It may also be useful to optimize the volume of cell lysis buffer used to lyse the cells following transfection, to ensure the release of transfected DNA from all the cells. It has been shown with plasmid DNA that the use of peptide scaffolds containing cationic peptides (which bind to the DNA) conjugated to a nonclassical nuclear localization sequence (NLS), greatly improves nuclear import and transfection efficiency (Subramanian, Ranganathan, & Diamond, 1999). These peptide scaffolds are commercially available as the reagent Nupherin™ (Biomol). In the future, the ability of this reagent to improve transfection of the substrate DNA, and to specifically target the DNA to the nucleus to monitor nuclear BER, may be investigated.

An unexpected observation from the transfection of control and substrate DNA was the coelution of the biotinylated DNA strand with the +8oxodG or -8oxodG DNA strand, following capture and denaturation (Figure 16A). This was however not observed during preliminary analysis of the bead capture and denaturation steps using the control DNA (Figure 13). We speculate that this may be due to the partial denaturation of the biotin moiety during repeated freeze-thaw of the control and substrate DNA for use in the optimization experiments. This may compromise the ability of the biotin-tagged substrate to bind strongly to the streptavidin-coated beads, thereby resulting in its elution following treatment with 0.1 M sodium hydroxide. If this were the case, then some of the

biotin-tagged substrate may have also been lost during the wash steps, which would then account for the low percentage recovery of the transfected DNA. This may be verified by analysis of the supernatant from the wash steps. In the future, aliquots of the substrate DNA may be prepared following quantification, to prevent the denaturation of the biotin moiety due to repeated freeze-thaw. It may also be useful to optimize the volume and concentration of sodium hydroxide, and the incubation time for the denaturation step, to ensure that the coelution of the biotinylated DNA strand was not due to the conditions used for these steps.

A commercially available competitive ELISA kit (Trevigen) was evaluated in this study for its specificity and efficiency in the detection of 8oxodG lesions on the +8oxodG DNA. The +8oxodG and -8oxodG DNA were used for this evaluation. The absorbance at 450 nm for the -8oxodG DNA was consistently at or near the readings obtained for the blank (0 ng/ml standard), while the readings for the +8oxodG DNA were lesser than the blank (lesser absorbance corresponds to more 8oxodG in competitive ELISA). This showed that the antibody specifically interacts with 8oxodG lesions. To determine conditions that improved specificity, the ELISA was performed using different blocking agents, primary antibody dilutions, and primary antibody incubation temperatures. It was observed that blocking the wells with 2% FBS gave high specificity when compared to 10% FBS and 1% BSA. The specificity was also highest when incubating the +8oxodG or -8oxodG DNA in the wells at room temperature, with a 1/250 dilution of the primary antibody. The ELISA detected 8oxodG lesions on the +8oxodG DNA with an efficiency of 46.3% and also demonstrated the ability to detect the lesions on the +8oxodG DNA in

a dose-dependent manner, in the presence of the -8oxodG DNA. Thus, when used in the BER assay, the 8oxodG ELISA would effectively quantify lesions on the unrepaired target DNA in the presence of repaired target DNA. Thus, the competitive 8oxodG ELISA (Trevigen) with some modifications, was found to be suitable for use in our assay to specifically detect and quantify 8oxodG lesions on the +8oxodG DNA of the oligonucleotide DNA substrate.

In summary, the design of a novel assay to measure the *in vivo* BER of 8oxodG lesions on an oligonucleotide DNA substrate was outlined in this study. The preparation of the substrate DNA and the optimal working conditions for the competitive ELISA were established. Preliminary experiments confirmed that the biotin-tagged substrate DNA can be successfully transfected into target cell cultures, and can be captured and purified using streptavidin-coated magnetic beads. By incubating cell cultures with the transfected substrate DNA for an increasing period of time, the steady-state measurements of BER activity in the cell may be obtained. In the future, the assay will have to be validated *in vivo* by comparing repair of the oligonucleotide DNA substrate in cell cultures that are known to possess functional BER versus those that do not. Since hOGG1 is a critical enzyme involved in the repair of 8oxodG lesions, an isogenic system consisting of hOGG1 knockout and hOGG1 wild-type cells may be used for validating the assay. To this end, stable isogenic cell lines for hOGG1 knockdown derived from MCF7 parental cell lines, have been developed at the Ford laboratory, and will be used to validate this assay in the future. Once validated, the assay may be used to confirm the

role of the BRCA1 protein, and investigate the role of other potential cancer-related proteins in the BER pathway.

CONCLUSION

The 8oxodG lesions are some of the most frequently observed products of oxidative DNA damage in cells. Unless repaired by the BER pathway, these lesions could result in AP sites, strand breaks, genetic instability, and carcinogenesis. Defects in BER may occur due to germ-line or somatic mutations in the genes coding for BER-associated proteins. Defective cellular BER may be detected using assays, most of which are performed in vitro using cell protein extracts and radiolabeled reagents. A novel in vivo HCR assay for BER was recently developed in our laboratory. In chapter one of this thesis, we described the use of the HCR assay in SUM149PT cells to investigate the role of the BRCA1 protein in BER. An approximately two-fold increase in BER levels in cells transfected with the *BRCA1*-wild type construct when compared to those transfected with the empty vector control was observed. This suggested that the BRCA1 protein was involved in the BER pathway.

In order to corroborate the findings from chapter one, another in vivo assay for BER was necessary. In chapter two of this thesis, we described our design and optimization of a novel in vivo assay for BER. This assay monitors BER in target cells using a biotin-tagged, double-stranded, 8oxodG containing oligonucleotide DNA substrate, and an 8oxodG ELISA. Our assay offers an advantage over existing assays in that it measures the kinetics of BER in vivo and it does not use radiolabeled reagents. In the future, following validation of this assay in vivo, it may be used to confirm the role of the BRCA1 protein in BER.

REFERENCES

- Achanta, G. & Huang, P. (2004). Role of p53 in sensing oxidative DNA damage in response to reactive oxygen species-generating agents. *Cancer Research*, 64, 6233-6239.
- Alli, E. (2006). [Host-cell reactivation assay]. Unpublished raw data.
- Alli, E. (2008). [Base excision DNA repair defects in basal-like and *BRCA1*-mutated breast cancer cells]. Unpublished raw data.
- Anson, R. M., Hudson, E., & Bohr, V. A. (2000). Mitochondrial endogenous oxidative damage has been overestimated. *The FASEB Journal*, 14, 355-360.
- Bae, I., Fan, S., Meng, Q., Rih, J. K., Kim, H. J., Kang, H. J., et al. (2004). BRCA1 induces antioxidant gene expression and resistance to oxidative stress. *Cancer Research*, 64, 7893-7909.
- Biade, D., Sobol, R. W., Wilson, S. H., & Matsumoto, Y. (1998). Impairment of proliferating cell nuclear antigen-dependent apurinic/apyrimidinic site repair on linear DNA. *Journal of Biological Chemistry*, 273, 898-902.
- Bjelland, S. & Seeberg, E. (2003). Mutagenicity, toxicity and repair of DNA base damage induced by oxidation. *Mutation Research*, 531, 37-80.
- Blagosklonny, M. V., An, W. G., Melillo, G., Nguyen, P., Trepel, J. B., & Neckers, L. M. (1999). Regulation of BRCA1 by protein degradation. *Oncogene*, 18, 6460-6468.
- Bochar, D. A., Wang, L., Beniya, H., Kinev, A., Xue, Y., & Lane, W. S. (2000). BRCA1 is associated with a human SWI/SNF-related complex: linking chromatin remodeling to breast cancer. *Cell*, 102, 257-265.

- Bogdan, C., Röllinghoff, M., & Diefenbach, A. (2000). Reactive oxygen and reactive nitrogen intermediates in innate and specific immunity. *Current Opinion in Immunology*, 12, 64-76.
- Brodie, S. G., Xu, X., Qiao, W., Li, W. M., Cao, L., & Deng, C. X. (2001). Multiple genetic changes are associated with mammary tumorigenesis in Brca1 conditional knockout mice. *Oncogene*, 20, 7514-7523.
- Budhram-Mahadeo, V., Ndisang, D., Ward, D., Weber, B. L., & Latchman, D. S. (1999). The Brn-3b POU family transcription factor represses expression of the *BRCA1* anti-oncogene in breast cancer cells. *Oncogene*, 18, 6684-6691.
- Cable, P. L., Wilson, C. A., Calzone, F. J., Rauscher, F. J., III, Scully, R., Livingston, D. M. et al. (2003). Novel consensus DNA-binding sequence for BRCA1 protein complexes. *Molecular Carcinogenesis*, 38, 85-96.
- Caldecott, K. W. (2003). The BRCT Domain: Signaling with Friends? *Science*, 302, 579 – 580.
- Cappelli, E., Degan, P., & Frosina, G. (2000). Comparative repair of the endogenous lesions 8-oxo-7,8-dihydroguanine (8-oxoG), uracil and abasic site by mammalian cell extracts: 8-oxoG is poorly repaired by human cell extracts. *Carcinogenesis*, 21, 1135-1141.
- Catteau, A. & Morris, J. R. (2002). *BRCA1* methylation: a significant role in tumor development? *Seminars in Cancer Biology*, 12, 359-371.
- Cheng, K. C., Cahill, D. S., Kasai, H., Nishimura, S., & Loeb, L. A. (1992). 8-Hydroxyguanine, an abundant form of oxidative DNA damage, causes G---T and A---C substitutions. *Journal of Biological Chemistry*, 267, 166-172.
- Collins, A. R., Cadet, J., Moller, L., Poulsen, H. E., & Vina, J. (2004). Are we sure we know how to measure 8-oxo-7,8-dihydroguanine in DNA from human cells? *Archives of Biochemistry and Biophysics*, 423, 57-65.

- Collins, A. R. & Dušinská, M. (2002). Oxidation of cellular DNA measured with the comet assay. *Methods in Molecular Biology*, 186, 147-160.
- Collins, A. R., Oscoz, A. A., Brunborg, G., Gaivão, I., Giovannelli, L., Kruszewski, M. et al. (2008). The comet assay: topical issues. *Mutagenesis*, 23, 143-151.
- Daniel, D. C. (2002). Highlight: BRCA1 and BRCA2 proteins in breast cancer. *Microscopy Research and Technique*, 59, 68-83.
- David, S. S., O'Shea, V. L., & Kundu, S. (2007). Base-excision repair of oxidative DNA damage. *Nature*, 447, 941-950.
- Degan, P., Bonassi, S., De Caterina, M., Korkina, L. G., Pinto, L., Scopacasa, F. et al. (1995). In vivo accumulation of 8-hydroxy-2'-deoxyguanosine in DNA correlates with release of reactive oxygen species in Fanconi's anaemia families. *Carcinogenesis*, 16, 735-742.
- Degan, P., Shigenaga, M. K., Park, E. M., Alperin, P. E., & Ames, B. N. (1991). Immunoaffinity isolation of urinary 8-hydroxy-2'-deoxyguanosine and 8-hydroxyguanine and quantitation of 8-hydroxy-2'-deoxyguanosine in DNA by polyclonal antibodies. *Carcinogenesis*, 12, 865-871.
- Deng, C. (2006). BRCA1- cell cycle checkpoint, genetic instability, DNA damage response and cancer evolution. *Nucleic Acids Research*, 34, 1416-1426.
- Dianov, G., Bischoff, C., Piotrowski, J., & Bohr, V. A. (1998). Repair pathways for processing of 8-oxoguanine in DNA by mammalian cell extracts. *Journal of Biological Chemistry*, 273, 33811-33816.
- Dizdaroglu, M. (2005). Base-excision repair of oxidative DNA damage by DNA glycosylases. *Mutation Research - Fundamental and Molecular Mechanisms of Mutagenesis*, 591, 45-59.

- Dulic, A., Bates, P. A., Zhang, X., Martin, S. R., Freemont, P. S., Lindahl, T. et al. (2001). BRCT domain interactions in the heterodimeric DNA repair protein XRCC1-DNA ligase III. *Biochemistry*, 40, 5906-5913.
- Easton, D. & Peto, J. (1990). The contribution of inherited predisposition to cancer incidence. *Cancer Surveys*, 9, 395-416.
- Elstrodt, F., Hollestelle, A., Nagel, J. H., Gorin, M., Wasielewski, M., Van den Ouweland, A. et al. (2006). *BRCA1* mutation analysis of 41 human breast cancer cell lines reveals three new deleterious mutants. *Cancer Research*, 66, 41-45.
- Floyd, R. A., Watson, J. J., Wong, P. K., Altmiller, D. H., & Rickard, R. C. (1986). Hydroxyl free radical adduct of deoxyguanosine: Sensitive detection and mechanisms of formation. *Free Radical Research Communications*, 1, 163-172.
- Fortini, P., Parlanti, E., Sidorkina, O. M., Laval, J., & Dogliotti, E. (1999). The type of DNA glycosylase determines the base excision repair pathway in mammalian cells. *Journal of Biological Chemistry*, 274, 15230-15236.
- Fortini, P., Pascucci, B., Parlanti, E., Errico, M. D., Simonelli, V., & Dogliotti, E. (2003). 8-Oxoguanine DNA damage: at the crossroad of alternative repair pathways. *Mutation Research*, 531, 127-139.
- Friedberg, E. C., Waker, G. C., Siede, W., Wood, R. D., Schultz, R. A., & Ellenberger, T. (2006a). DNA damage. In *DNA repair and mutagenesis* (2nd ed., pp. 9-57). Washington, DC: American Society for Microbiology Press.
- Friedberg, E. C., Waker, G. C., Siede, W., Wood, R. D., Schultz, R. A., & Ellenberger, T. (2006b). Base excision repair. In *DNA repair and mutagenesis* (2nd ed., pp. 187-191). Washington, DC: American Society for Microbiology Press.
- Fromme, J. C. & Verdine, G. L. (2004). Base Excision Repair. *Advances in Protein Chemistry*, 69, 1-41.

- Hartman, A. R. & Ford, J. M. (2002). BRCA1 induces DNA damage recognition factors and enhances nucleotide excision repair. *Nature Genetics*, 32, 180-184.
- Hazra, K., Izumi, T., Maiti, L., Floyd, R. A., & Mitra, S. (1998). The presence of two distinct 8-oxoguanine repair enzymes in human cells: their potential complementary roles in preventing mutation. *Nucleic Acids Research*, 26, 5116-5122.
- Heiman, M. (1997). Webcutter (Version 2.0) [Web-based computer software]. Accessed January 20, 2007, from <http://rna.lundberg.gu.se/cutter2/>
- Hirano, T. (2008). Repair system of 7, 8-dihydro-8-oxoguanine as a defense line against carcinogenesis. *Journal of Radiation Research*, 49, 329-340.
- Höss, M., Jaruga, P., Zastawny, T. H., Dizdaroglu, M., & Pääbo, S. (1996). DNA damage and DNA sequence retrieval from ancient tissues. *Nucleic Acids Research*, 24, 1304-1307.
- Hou, E. W., Prasad, R., Asagoshi, K., Masaoka, A., & Wilson, S. H. (2007). Comparative assessment of plasmid and oligonucleotide DNA substrates in measurement of in vitro base excision repair activity. *Nucleic Acids Research*, 35, e112.
- Kinzler, K. W. & Vogelstein, B. (1997). Cancer-susceptibility genes. Gatekeepers and caretakers. *Nature*, 386, 761-763.
- Krokan, H. E., Nilsen, H., Skorpen, F., Otterlei, M., & Slupphaug, G. (2000). Base excision repair of DNA in mammalian cells. *FEBS Letters*, 476, 73-77.
- Lakowicz, J. R. Mechanisms and dynamics of fluorescence quenching. In *Principles of fluorescence spectroscopy* (3rd ed., pp. 341). New York, NY: Springer.
- Lane, T. F. (2004). BRCA1 and transcription. *Cancer Biology and Therapy*, 3, 528-533.

- Lechardeur, D., Sohn, K. J., Haardt, M., Joshi, P. B., Monck, M., Graham, R. W. et al. (1999). Metabolic instability of plasmid DNA in the cytosol: a potential barrier to gene transfer. *Gene Therapy*, 6, 482-497.
- Li, Y., Dowbenko, D., & Lasky, L. A. (2002). KT/PKB phosphorylation of p21Cip/WAF1 enhances protein stability of p21Cip/WAF1 and promotes cell survival. *Journal of Biological Chemistry*, 277, 11352-11361.
- Lindahl, T. (1974). An N-glycosidase from *Escherichia coli* that releases free uracil from DNA containing deaminated cytosine residues. *Proceedings of the National Academy of Sciences U.S.A.*, 71, 3649-3653.
- Lindahl, T. (1993). Instability and decay of the primary structure of DNA. *Nature*, 362, 709-715.
- Malins, D. C. & Haimanot, R. (1991). Major alterations in the nucleotide structure of DNA in cancer of the female breast. *Cancer Research*, 51, 5430-5432.
- McKelvey-Martin, V. J., Green, M. H. L., Schmezer, P., Pool-Zoberl, B. L., & Collins, A. (1993). The single cell gel electrophoresis assay (comet assay): A European review. *Mutation Research*, 288, 47-63.
- Miki, Y., Swensen, J., Shattuck-Eidens, D., Futreal, P. A., Harshman, K., Tavtigian, S. et al. (1994). A strong candidate for the breast and ovarian cancer susceptibility gene *BRCA1*. *Science*, 266, 66-71.
- Mitra, S., Boldogh, I., Izumi, T., & Hazra, T. K. (2001). Complexities of the DNA base excision repair pathway for repair of oxidative DNA damage. *Environmental and Molecular Mutagenesis*, 38, 180-190.
- Monteiro, A. N. (2000). BRCA1: exploring the links to transcription. *Trends in Biochemical Sciences*, 25, 469-474.
- Musarrat, J. & Wani, A. A. (1994). Quantitative immunoanalysis of promutagenic 8-hydroxy-2'-deoxyguanosine in oxidized DNA. *Carcinogenesis*, 15, 2037-2043.

- Neeley, E. L. & Essigmann, J. M. (2006). Mechanisms of formation, genotoxicity, and mutation of guanine oxidation products. *Chemical Research in Toxicology*, 19, 491-505.
- Neve, R. M., Chin, K., Fridlyand, J., Yeh, J., Baehner, F. L., Fevr, T. et al. (2006). A collection of breast cancer cell lines for the study of functionally distinct cancer subtypes. *Cancer Cell*, 10, 515-527.
- Nilsen, H. & Krokan, H. E. (2001). Base excision repair in a network of defense and tolerance. *Carcinogenesis*, 22, 987-998.
- Pacifici, R. E. & Davies, K. J. (1991). Protein, lipid and DNA repair systems in oxidative stress: the free-radical theory of aging revisited. *Gerontology*, 37, 166-180.
- Park, J. H., Gopishetty, S., Szewczuk, L. M., Troxel, A. B., Harvey, R. G., & Penning, T. M. (2005). Formation of 8-oxo-7,8-dihydro-2'-deoxyguanosine (8-oxo-dGuo) by PAH o-quinones: Involvement of reactive oxygen species and copper(II)/copper(I) redox cycling. *Chemical Research in Toxicology*, 18, 1026-1037.
- Paz-Elizur, T., Krupsky, M., Blumenstein, S., Elinger, D., Schechtman, E., & Livneh, Z. (2003). DNA repair activity for oxidative damage and risk of lung cancer. *Journal of the National Cancer Institute*, 95, 1312-1319.
- Perrin-Vidoz, L., Sinilnikova, O. M., Stoppa-Lyonnet, D., Lenoir, G. M., & Mazoyer, S. (2002). The nonsense-mediated mRNA decay pathway triggers degradation of most *BRCA1* mRNAs bearing premature termination codons. *Human Molecular Genetics*, 11, 2805-2814.
- Poulsen, H. E., Prieme, H., & Loft, S. (1998). Role of oxidative DNA damage in cancer initiation and promotion. *European Journal of Cancer Prevention*, 7, 9-16.
- Rasband, W. (2006). Image J (Version 1.37) [Computer software]. National Institutes of Health, USA. Retrieved May 30, 2007, from <http://rsbweb.nih.gov/ij/>

- Ravanat, J. L., Douki, T., Duez, P., Gremaud, E., Herbert, K., Hofer, T. et al. (2002). Cellular background level of 8-oxo-7,8-dihydro-2'-deoxyguanosine: an isotope based method to evaluate artefactual oxidation of DNA during its extraction and subsequent work-up. *Carcinogenesis*, 23, 1911–1918.
- Rosenquist, T. A., Zharkov, D. O., & Grollman, A. P. (1997). Cloning and characterization of a mammalian 8-oxoguanine DNA glycosylase. *Proceedings of the National Academy of Sciences U.S.A*, 94, 7429–7434.
- Sambrook, J., Fritsch, E. F., & Maniatis, T. (1989). Preparation of reagents and buffers used in molecular cloning. In N. Ford, C. Nolan & M. Ferguson (Eds.), *Molecular cloning: A laboratory manual* (pp. B24). New York: Cold Spring Harbor Laboratory Press.
- Schagen, F. H., Moor, A. C., Cheong, S. C., Cramer, S. J., Van Ormondt, H., Van der Eb, A. J. et al. (1999). Photodynamic treatment of adenoviral vectors with visible light: an easy and convenient method for viral inactivation. *Gene Therapy*, 6, 873-881.
- Schneider, J. E., Price, S., Maidt, L., Gutteridge, J. M. C., & Floyd, R. A. (1990). Methylene blue plus light mediated 8-hydroxy 2'-deoxyguanosine formation in DNA preferentially over strand breakage. *Nucleic Acids Research*, 18, 631-635.
- Scully, R., Ganesan, S., Brown, M., De Caprio, J. A., Cannistra, S. A., Feunteun, J. et al. (1996). Location of BRCA1 in human breast and ovarian cancer cells. *Science*, 272, 123-126.
- Scully, R., Ganesan, S., Vlasakova, K., Chen, J., Socolovsky, M., & Livingston, D. M. (1999). Genetic analysis of BRCA1 function in a defined tumor cell line. *Molecular Cell*, 4, 1093–1099.
- Scully, R., Xie, A., & Nagaraju, G. (2004). Molecular functions of BRCA1 in DNA damage response. *Cancer Biology and Therapy*, 3, 521-527.
- Seeberg, E., Eide, L., & Bjørås, M. (1995). The base excision repair pathway. *Trends in Biochemical Science*, 20, 391–397.

- Shibutani, S., Takeshita, M., & Grollman, A. P. (1991). Insertion of specific bases during DNA synthesis past the oxidation damaged base 8-oxodG. *Nature*, 349, 431–434.
- Sipe, H. J. J., Jordan, S. J., Hanna, P. M., & Mason, R. P. (1994). The metabolism of 17 β estradiol by lactoperoxidase: a possible source of oxidative stress in breast cancer. *Carcinogenesis*, 15, 2637-2643.
- Starita, L. M. & Parvin, J. D. (2003). The multiple nuclear functions of BRCA1: transcription, ubiquitination and DNA repair. *Current Opinion in Cell Biology*, 15, 345-350.
- Steenken, S. & Jovanovic, S. V. (1997). How easily oxidizable is DNA? One-electron reduction potentials of adenosine and guanosine radicals in aqueous solution. *Journal of the American Chemical Society*, 119, 617-618.
- Stover, J. S., Ciobanu, M., Cliffl, D. E., & Rizzo, C. J. (2007). Chemical and electrochemical oxidation of C8-arylamine adducts of 2'-deoxyguanosine. *Journal of the American Chemical Society*, 129, 2074-2081.
- Subramanian, A., Ranganathan, P., & Diamond, S. L. (1999). Nuclear targeting peptide scaffolds for lipofection of nondividing mammalian cells. *Nature Biotechnology*, 17, 873 – 877.
- Tirkkonen, M., Johannsson, O., Agnarsson, B. A., Olsson, H., Ingvarsson, S., Karhu, R. et al. (1997). Distinct somatic genetic changes associated with tumor progression in carriers of *BRCA1* and *BRCA2* germ-line mutations. *Cancer Research*, 57, 1222–1227.
- Toyokuni, S., Okamoto, K., Yodoi, J., & Hiai, H. (1995). Persistent oxidative stress in cancer. *FEBS Letters*, 358, 1-3.
- Venkitaraman, A. R. (2001). Functions of BRCA1 and BRCA2 in the biological response to DNA damage. *Journal of Cell Science*, 114, 3591-3598.

- Vidal, A. E., Hickson, I. D., Boiteux, S., & Radicella, J. P. (2001). Mechanism of stimulation of the DNA glycosylase activity of hOGG1 by the major human AP endonuclease: bypass of the AP lyase activity step. *Nucleic Acids Research*, 29, 1285–1292.
- Wang, Y., Cortez, D., Yazdi, P., Neff, N., Elledge, S. J., & Qin, J. (2000). BASC, a super complex of BRCA1-associated proteins involved in the recognition and repair of aberrant DNA structures. *Genes and Development*, 14, 927-939.
- Weaver, Z., Montagna, C., Xu, X., Howard, T., Gadina, M., Brodie, S. G., et al. (2002). Mammary tumors in mice conditionally mutant for Brcal exhibit gross genomic instability and centrosome amplification yet display a recurring distribution of genomic imbalances that is similar to human breast cancer. *Oncogene*, 21, 5097–5107.
- Xu, X., Wagner, K. U., Larson, D., Weaver, Z., Li, C., Ried, T., et al. (1999). Conditional mutation of Brcal in mammary epithelial cells results in blunted ductal morphogenesis and tumor formation. *Nature Genetics*, 22, 37-43.
- Yarden, R. I. & Papa, M. Z. (2006). BRCA1 at the crossroad of multiple cellular pathways: approaches for therapeutic interventions. *Molecular Cancer Therapeutics*, 5, 1396-1404.
- Yin, B., Whyatt, R. B., Perera, F. P., Randall, M. C., Cooper, T. B., & Santella, R. M. (1995). Determination of 8-hydroxydeoxyguanosine by an immunoaffinity chromatography-monoclonal antibody-based ELISA. *Free Radical Biology and Medicine*, 18, 1023–1032.
- Zhang, H., Somasundaram, K., Peng, Y., Tian, H., Zhang, H., Bi, D. et al. (1998). BRCA1 physically associates with p53 and stimulates its transcriptional activity. *Oncogene*, 16, 1713-1721.
- Zhang, J., & Powell, S. N. (2005). The role of the BRCA1 tumor suppressor in DNA double strand break repair. *Molecular Cancer Research*, 3, 531-539.

Zhuang, J., Zhang, J., Willers, H., Wang, H., Chung, J. H., Van Gent, D. C. et al. (2006). Checkpoint kinase 2-mediated phosphorylation of BRCA1 regulates the fidelity of nonhomologous end-joining. *Cancer Research*, 66, 1401-1408.

Zipper, H., Brunner, H., Bernhagen, J., & Vitzthum, F. (2004). Investigations on DNA intercalation and surface binding by SYBR Green I, its structure determination and methodological implications. *Nucleic Acids Research*, 32, e103.